

Award Number 02HQGR0015
The University of Arizona

**GROUND FAILURE RESULTING FROM THE
2001 NISQUALLY EARTHQUAKE**

Dr. Scott M. Merry, PE, GE

Associate Professor

Department of Civil Engineering
School of Engineering and Computer Science
University of the Pacific
3601 Pacific Avenue
Stockton, California, 95211

Email: smerry@pacific.edu

Research supported by the U.S. Geological Survey (USGS), Department of the Interior, under award number 02HQGR0015. The views and conclusions contained in this document are those of the authors and should not be interpreted as necessarily representing the official policies, either expressed or implied, of the U.S. Government.

Ground Failure Resulting from the 2001 Nisqually Earthquake

Grant Award 02HQGR0015

Principal Investigator: Dr. Scott Merry, PE, GE¹

KEYWORDS

Liquefaction, CPT, SPT, Energy

TECHNICAL ABSTRACT

A study of liquefaction at three sites in the Seattle/Olympia area during the 2001 Nisqually earthquake is presented. Results of this case history study include: (a) cone penetration test (CPT) data for each of the sites where surficial evidence of liquefaction was observed. In some of the sites, additional CPT data was recorded where evidence of liquefaction was not as clearly established; (b) standard penetration test (SPT) data for each of the sites; (c) energy measurements recorded for standard penetration tests; and (d) a liquefaction evaluation based on CPT and SPT data documented how the test data correlated with the observed liquefaction. Relative to the SPT, the CPT profiling provided a more reliable method for predicting the performance of the poorly compacted fills. Additional discussions include the differences between them and advantages and disadvantages of both methods.

Standard penetration resistance testing proved to be problematic due to a wide variation in energy applied to the drill rods. The commercially-available autotrip hammer provided a relative energy (ratio of measured energy to that expected for the standardized test) of approximately 93 percent or greater. This was due to a design flaw in the hammer that provided a fall height of 35 inches rather than the prescribed 30 inches. Having discovered this, conventional rope and cathead methods were used. Several factors (worn rope, rusty cathead, operator variance) provided relative energy values that varied from less than 40 percent to approximately 55 percent. Given the variability of the latter method, discerning a consistent energy correction to establish a normalized blowcount, $N_{1(60)}$ without continuous monitoring of the blowcount energies was not possible.

¹ Associate Professor, Department of Civil Engineering, School of Engineering and Computer Science, University of the Pacific, 3601 Pacific Avenue, Stockton, California, 95211, smerry@pacific.edu.

Ground Failure Resulting from the 2001 Nisqually Earthquake

Grant Award 02HQGR0015

Principal Investigator: Scott Merry, PhD, PE, GE¹

KEYWORDS

Liquefaction, CPT, SPT, Energy

NONTECHNICAL ABSTRACT

A study of liquefaction at three sites in the Seattle/Olympia area during the 2001 Nisqually earthquake is presented. Results of this case history study include: (a) cone penetration test (CPT) data for each of the sites where surficial evidence of liquefaction was observed. In some of the sites, additional CPT data was recorded where evidence of liquefaction was not as clearly established; (b) standard penetration test (SPT) data for each of the sites; (c) energy measurements recorded for standard penetration tests; and (d) a liquefaction evaluation based on CPT and SPT data documented how the test data correlated with the observed liquefaction. Additional discussions include the differences between them and advantages and disadvantages of both methods.

¹ Associate Professor, Department of Civil Engineering, School of Engineering and Computer Science, University of the Pacific, 3601 Pacific Avenue, Stockton, California, 95211, smerry@pacific.edu.

Ground Failure Resulting from the 2001 Nisqually Earthquake

Scott Merry, PhD, PE, GE¹, Vasco Duke, PE², and Juan Lopez, PE³

ABSTRACT

A study of liquefaction at three sites in the Seattle/Olympia area during the 2001 Nisqually earthquake is presented. Results of this case history study include: (a) cone penetration test (CPT) data for each of the sites where surficial evidence of liquefaction was observed. In some of the sites, additional CPT data was recorded where evidence of liquefaction was not as clearly established; (b) standard penetration test (SPT) data for each of the sites; (c) energy measurements recorded for standard penetration tests; and (d) a liquefaction evaluation based on CPT and SPT data documented how the test data correlated with the observed liquefaction. Additional discussions include the differences between them and advantages and disadvantages of both methods.

CHAPTER 1: INTRODUCTION TO LIQUEFACTION

1.1 Introduction

Many of the procedures the Civil Engineering profession relies upon in evaluating earthquake hazards are empirically based. For example, many of the prevailing liquefaction triggering and lateral spread displacement evaluation procedures are based upon well-documented case histories from past earthquakes. These procedures form the basis for many of the regional and site-specific hazard assessment methodologies in earthquake engineering. These commonly used empirically based seismic assessment procedures require re-evaluation and updating as important case histories emerge. The observed ground failures in the Olympia and Seattle areas during the February 28, 2001 Nisqually Earthquake provide an exceptional opportunity to advance the state-of-practice in assessing the response of soils to low intensity, long duration earthquake motions.

The 2001 Nisqually earthquake caused extensive liquefaction throughout the cities of Seattle, Tacoma, and Olympia in Washington. Liquefaction evidence was found in several sites of these cities; with structural damage occurring at several locations while essentially no damage occurred at others. Overviews of the damage caused by this earthquake can be found in Bray et al. (2001) "Some Observations of Geotechnical Aspects of the February 28, 2001, Nisqually Earthquake in Olympia, South Seattle, and Tacoma, Washington".

¹ Associate Professor, Department of Civil Engineering, School of Engineering and Computer Science, University of the Pacific, 3601 Pacific Avenue, Stockton, California, 95211, smerry@pacific.edu.

² Project Engineer, URS Corporation, 7650 W Courtney Campbell Causeway, Tampa, FL 33607, vasco_duke@urscorp.com.

³ Intermediate Geotechnical Engineer, Golder Associates Ltd., 102, 2535 - 3rd Avenue S.E., Calgary, Alberta, Canada T2A 7W5, Juan_Lopez@golder.com

A case-history study of liquefaction-related effects in the Seattle/Olympia area in Washington during the 2001 Nisqually earthquake is presented here. Four sites were investigated: The Port of Olympia, a lateral spreading in Martin Way Avenue at Olympia, a building failure south of downtown Seattle, and the Deschutes Parkway at Olympia. This paper contains a full analysis of the liquefaction potential of these sites based on SPT, CPT, and shear wave velocity tests. In some of the sites the shear wave velocity was not recorded. In addition to the liquefaction analysis the paper describes briefly the geologic setting of the sites, soil profiles based on Standard penetration tests, CPT tests, and soil samples recovered at the sites.

Several cases of ground failure and building damage near Olympia and an area south of downtown Seattle could provide exceptional field performance data on critical seismic geotechnical phenomena, if these cases are well documented. Documentation of the ground failure at these sites and development of good subsurface characterizations will allow these important case histories to be incorporated into the existing databases on which empirical procedures are based.

The goals of this study will be met in part by completing documentation of these important case records through CPT and SPT profiling, soil index testing, and cyclic simple shear strength testing in the laboratory.

1.2 An Introduction to Liquefaction

Liquefaction is a phenomenon in which the strength and stiffness of a soil is reduced by earthquake shaking or other rapid loading. Liquefaction and related phenomena have been responsible for tremendous amounts of damage in historical earthquakes around the world.

Liquefaction occurs in saturated soils, that is, soils in which the space between individual particles is completely filled with water. This water exerts a pressure on the soil particles that influences how tightly the particles themselves are pressed together. Prior to an earthquake, the water pressure is relatively low or in hydrostatic pressure. However, earthquake shaking can cause the water pressure to increase to the point where the soil particles can readily move with respect to each other or hence behave as a liquid.

Earthquake shaking often triggers this increase in water pressure, but construction related activities such as blasting could also cause an increase in water pressure. When liquefaction occurs, the strength of the soil decreases and, the ability of a soil deposit to support foundations for buildings and bridges, or any other type of structure is reduced as seen in Figure 1-1. Figure 1-1 shows the overturned apartment complex buildings after the Niigata earthquake in 1964.

Liquefaction is defined as the transformation of a granular material from a solid to a liquefied state as a consequence of increased pore water pressure and reduced effective stress.

Liquefaction occurs when the increase in water pressure reduces the contact between particles (effective stress) as seen in Figure 1-2. The reduction in effective stress causes the soil to behave temporarily as a liquid, and the soil particles are then able to rearrange themselves causing settlement, lateral spreading or in some cases, where the pore water pressure is very high, even sand boils.



Figure 1-1: Photograph from Niigata, Japan following the 1964 Niigata earthquake (photo credit: National Geophysical Data Center).

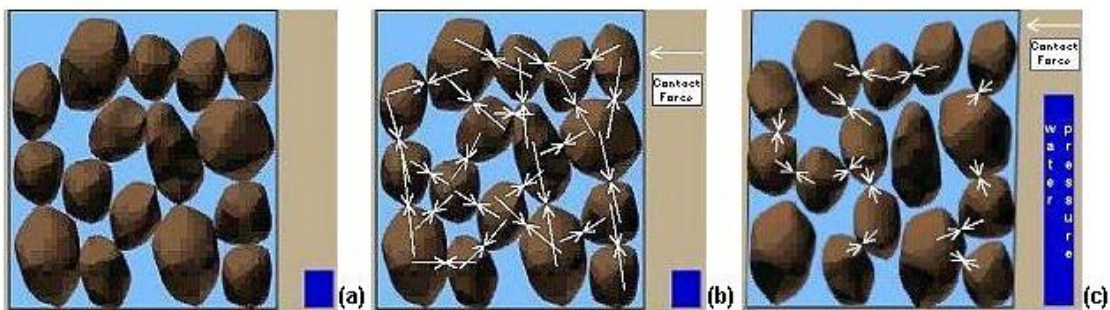


Figure 1-2: Liquefaction Process, (a) soil conditions at rest, (b) contact forces between particles at rest, and (c) contact forces after increased water pressure during liquefaction.

1.3 Factors affecting Liquefaction Potential

Several investigations (e.g., Seed and Idriss 1971, Seed (1979), Seed and Idriss (1982), and Seed et al. 1985, and Seed et al. 1994) have noted that there are five very important factors affecting liquefaction potential. The significant factors include:

- **Soil Type:** For cohesionless soils, the soil type is perhaps most easily characterized by the grain size distribution. There is some evidence to show that uniformly graded materials are more susceptible to liquefaction than well graded materials and that for uniformly graded soils, fine sands tend to liquefy more easily than do coarse sands, gravelly soils, silts, or clays.
- **Relative Density or Void Ratio:** The relative density or void ratio of soils clearly affects their liquefaction potential. In any given earthquake or dynamic loading of soils, loose sands (low relative density) may liquefy but the same materials in a denser condition may not.

- Initial Confining Pressure: There is considerable evidence showing that the liquefaction potential of a soil is reduced by an increase in confining pressure. This indicates that material at shallow depths (low confining stresses) may liquefy, and that same material a little deeper may not liquefy due to higher confining stresses.
- Intensity of Ground Shaking: For a soil in a given condition and under a given confining pressure, the vulnerability to liquefaction during an earthquake depends on the magnitude of the stresses or strains induced in it by the earthquake; these in turn are related to the intensity of ground shaking.
- Duration of Ground Shaking: The duration of ground shaking is a significant factor in determining liquefaction potential because it determines in a general way the number of significant stress or strain cycles to which a soil is subjected. All laboratory studies of soil liquefaction under cyclic loading conditions show that for any given stress or strain level, the onset of liquefaction depends on the application of a requisite number of stress or strain cycles.

CHAPTER 2: FIELD WORK AND LABORATORY TESTING

2.1 SPT Field Work

The standard penetration tests and associated fieldwork was completed by Geo-Tech Explorations, Inc. (Geo-Tech) of Seattle, WA. The drilling was done following ASTM D 6066-96 (*Standard Practice for Determining the Normalized Penetration Resistance of Sands for Evaluation of Liquefaction Potential*). Notes were taken regarding specific details of every operation.

The methods of ASTM D 6066-96 were followed with the following clarifications or exceptions. The drill rig was equipped with a mud rotary drill. All drilling was completed with a 4.875-inch diameter tri-cone bit (Figure 2-1) and NWJ rods.

At all of the sites CPT tests were conducted prior to the Standard penetration tests. The soil profiles provided by the CPT test results were evaluated to determine the depths for the Standard penetration tests. The Standard penetration tests were completed using both an auto-trip hammer and a safety hammer operated by a rope and cathead drop system. Both hammers included a 140 lb weight. Although the standard drop distance for these hammers is supposed to be 30 inches, it was discovered through a dynamic energy evaluation (discussed later) that the auto-trip hammer supplied by Geo-Tech had a 33-inch drop height. A full description of the hammer can be seen in Figure 2-2. Although AWJ rods are preferred for liquefaction evaluation, NWJ rods were supplied by Geo-Tech. NWJ drill rods are larger in diameter and heavier than AWJ rods; hence, they may provide lower field blow counts compared to when AWJ rods are used in the same location and depth.



Figure 2-1: 4.875-inch diameter tri-cone bit used for SPT boreholes in this study.

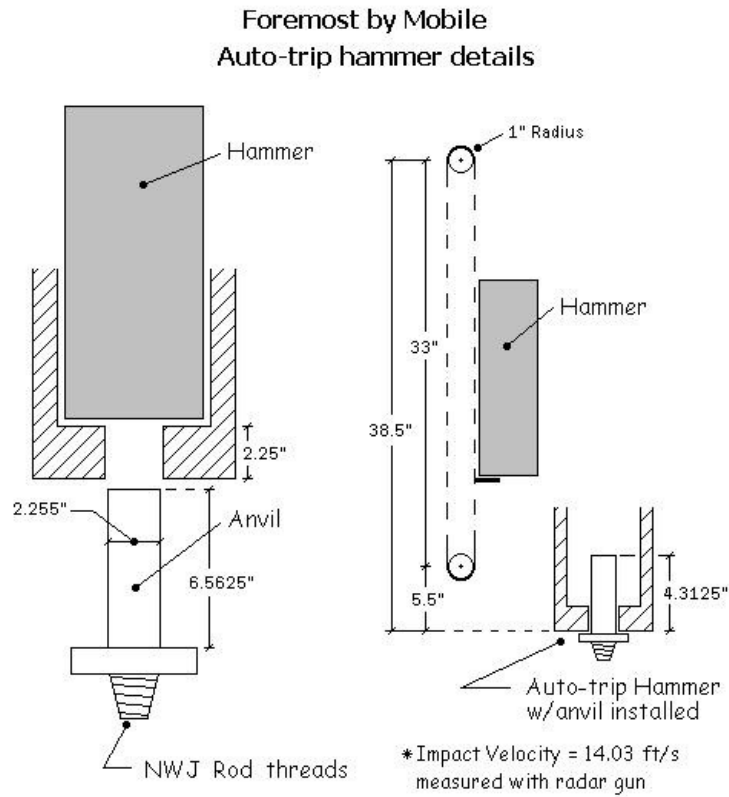


Figure 2-2: Auto-trip Hammer details and measurements.

The Split spoon sampler provided by Geo-Tech was a 1.5 feet long split spoon sampler. During the first few Standard penetration tests, a catcher was used because they generally help in the recovery of sandy samples, which were expected at these sites. However, in these early tests, very little recovery was found and hence, an idea of not using the catchers was proposed. Following the removal of the catchers, a very limited loss of recovery was experienced. An 18-inch long split spoon sampler was used without liners (see Figure 2-3).



Figure 2-3: Split spoon sampler used for standard penetration testing.

Besides the description and details recorded on the hammer, Robert Miner Dynamic Testing, Inc. recorded energy transmission data. A report was then received that included all the energy readings. This included the results of separate tests performed on the fall height of the auto-trip hammer. The results of the hammer-specific tests showed a hammer-anvil impact velocity of 14.03 feet per second (ft/s), as well as the blows per minute on both hammers. With this information a statistical analysis was conducted to determine the average energy transmission on both hammers. Dynamic energy measurements were carried out on only one borehole and these measurements were then used to perform the energy corrections on each of the subsequent boreholes. The energy transmission average on the auto-trip hammer was measured to be approximately 98% and 41% for the safety hammer. Additionally, the safety hammer using a rope and cathead had a significant amount of variation in the measured energies. The safety hammer system was marginal for being used on this project since ASTM D 6066-96 states that hammer systems that deliver a drill rod energy ratio, ER, of less than 40% should not be used. This low energy transfer seen in the cathead-rope system may have been caused due to friction between the rope and the cathead, humidity of the rope, or short-stroking of the rope by the operator. The blow counts per minute came out to be in

the average of 28 blows per minute. It is desired to apply blows at a rate of 20 to 40 blows per minute.

The drilling fluid used with the mud-rotary unit was bentonite quick gel drilling mud. The drilling fluid level within the borehole was maintained above the in situ piezometric water level. This precaution was taken for the stability of the borehole. Failure to maintain hydrostatic balance in the borehole can cause heaving or failure of the borehole. This notice should also be taken into account when sand layers under extreme artesian pressure are encountered.

Per ASTM D 6066-96, standard penetration testing should not be performed continuously on a borehole. The minimum recommended cleanout interval is 1.0 feet. If the cleanout interval is reduced to less than 1.0 feet, notice should be taken that the drill hole quality is maintained. This statement was initially overlooked in the first borehole at the South Seattle Site, leading to possibly inaccurate blow counts on the first 10 feet of the borehole. After this oversight was noted, another borehole was drilled five feet away in order to record new SPT blow counts over the upper 10 feet.

Three markings, each 6 inches (15 cm) apart, were applied to the drilling rods after the split spoon sampler had been lowered down inside the borehole. The penetration blow counts were recorded at each 6-inch interval. The N value (blow count) is defined as the number of blows of a 140 lb hammer falling 30 inches required to produce 1 foot of penetration of a specified 2-inch outside diameter, 1.375-inch inside diameter sampler into soil, after an initial 0.5 foot seating. This N value was then calculated adding the blow counts from the last two segments of the penetration length, which is from 0.5-1.0 feet and from 1.0-1.5 feet.

Once the standard penetration tests were performed and the split spoon sampler retrieved, the length of sample recovered was recorded, as was a brief visual description of the soils obtained in the sample. Slough and cuttings in the recovery length were not included. In some cases where different soil types were observed within the same sample, notes were taken and separated for later soil classification in the laboratory. This turned out to be very important since in just over a 6-inch segment, fines content of the sample could vary from 9 to 26 percent.

When the entire borehole had been logged and tested, it was backfilled with the use of bentonite chips. The samples were labeled and placed in Ziploc bags for later laboratory work. The borehole was then positioned using a Garmin III+ that recorded the global positioning system (GPS) coordinates of the hole. Boreholes could then be located in available maps for documentation of the site.

2.2 CPT Field Work

Cone Penetrometer Testing (CPT) is performed by hydraulically advancing a cone penetrometer rod into the ground while collecting real-time data. The data collected via down-hole instrumentation represents the soil responses (as the rod is advanced) in relation to tip resistance, friction sleeve resistance and pore pressures. Other information like soil resistivity, Shear and Compression waves velocity can be recorded depending on the cone penetrometer used.

An on-board CPT computer collects and displays real-time data enabling an accurate, on-site, subsurface representation including groundwater properties.

A primary advantage of the CPT is that a nearly continuous profile of penetration resistance is developed for stratigraphic interpretation. The CPT results are generally more consistent and repeatable than results from other penetration tests. The continuous profile also allows a more detailed definition of soil layers than other exploration techniques. This stratigraphic capability makes the CPT particularly advantageous for developing liquefaction-resistance profiles. Interpretations based on the CPT, however, must be verified with a few well-placed boreholes preferably with standard penetration tests, to confirm soil types and further verify liquefaction-resistance interpretations.

The CPT profiling was performed by Northwest Cone Exploration, Inc. The instrument used in our investigation was a Hogentogler 10-ton electronic subtraction cone. Table 2-1 lists the specifications of the equipment used. Figure 2-4 shows a description of the cone penetrometer used for the field investigations.

Table 2-1: Specifications of the Cone Penetrometer used in field tests.

Tip Area	10 cm ²
Internal Angle of Cone	60°
Sleeve Area	150 cm ²
Penetration Speed	2 cm/s
Measurement Interval	At every 5 cm
Rod Interval length	100 cm

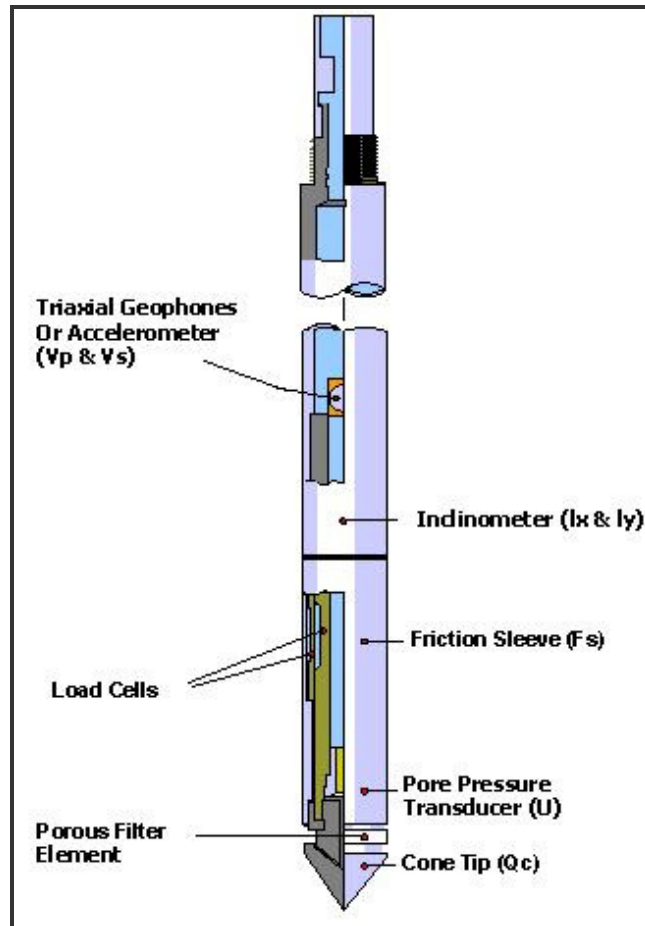


Figure 2-4: Sketch of Cone Penetrometer used in field explorations.

The length of the rod increment used was 100 cm and the depth interval at which the tip resistance, sleeve friction and pore water pressure were measured was 5 cm. The penetration speed was approximately kept at 2 cm/s.

CHAPTER 3: LIQUEFACTION EVALUATION

3.1 Introduction

Over the past 25 years a methodology termed the “simplified procedure” has evolved as a standard of practice for evaluating the liquefaction resistance of soils. Following the two earthquakes in 1964 (Alaska and Niigata, Japan), Seed and Idriss (1971) developed and published the basic “simplified procedure”. This procedure has been modified and improved periodically since that time (e.g., Seed 1979, Seed and Idriss 1982, and Seed et al. 1985). As of the late 1990s, a panel of experts convened and summarized the (then) state-of-the-art in Youd et al. (2001).

The simplified procedure was developed from empirical evaluations of field observations and field and laboratory test data. Field evidence of liquefaction generally consisted of superficial observations of sand boils, ground fissures, or lateral spreads.

When liquefaction occurs, increased pore water pressure is induced by the tendency of granular materials to compact when subjected to cyclic shear deformations. The change of state occurs most readily in loose to moderately dense granular soils with poor drainage, such as silty sands or sands and gravels capped by or containing seams of impermeable sediment. As liquefaction occurs, the soil stratum softens, allowing large cyclic deformations to occur. In loose materials, the softening is also accompanied by a loss of shear strength that may lead to large shear deformations or even flow failure under moderate to large shear stresses, such as beneath a foundation or sloping ground. In moderately dense to dense materials, liquefaction leads to transient softening and increased cyclic shear strains, but a tendency to dilate during shear inhibits major strength loss and large ground deformations. A condition of cyclic mobility or cyclic liquefaction may develop following liquefaction of moderately dense granular materials. Beneath gently sloping to flat ground, liquefaction may lead to ground oscillation or lateral spread as a consequence of either flow deformation or cyclic mobility. Loose soils also compact during liquefaction and reconsolidation, leading to ground settlement. Sand boils may also erupt as excess pore water pressures dissipate.

3.2 Cyclic Stress Ratio (CSR) and Cyclic Resistance Ratio (CRR)

To estimate the liquefaction resistance of a soil, two variables are required: the seismic demand on a soil layer, expressed in terms of cyclic stress ratio (CSR); and the capacity of the soil to resist liquefaction, expressed in terms of cyclic resistance ratio (CRR).

3.2.1 Evaluation of CSR

Seed and Idriss (1971) formulated the following equation for calculation of the cyclic stress ratio:

$$CSR = \left(\frac{\tau_{av}}{\sigma'_{vo}} \right) = 0.65 \left(\frac{a_{max}}{g} \right) \left(\frac{\sigma_{vo}}{\sigma'_{vo}} \right) r_d$$

where

a_{max} = peak acceleration at the ground surface generated by the earthquake:

g = acceleration of gravity

σ'_{vo} = effective vertical overburden stress

σ_{vo} = total vertical overburden stress

r_d = stress reduction coefficient.

The stress reduction coefficient (r_d) accounts for flexibility of the soil profile and it increases with depth. This coefficient is calculated with an equation that is an approximation of the mean values of the r_d versus depth curves generated by Seed and Idriss (1971) as seen in Figure 3-1 (Youd et al. 2001).

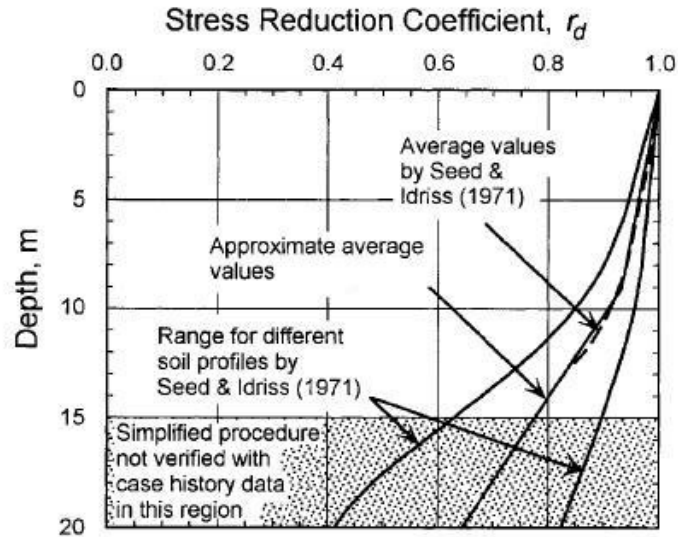


Figure 3-1: R_d versus depth curves developed by Seed and Idriss (1971) with added mean-value lines.

$$r_d = \frac{1.000 - 0.4113z^{0.5} + 0.04052z + 0.001753z^{1.5}}{1.000 - 0.4177z^{0.5} + 0.05729z - 0.006205z^{1.5} + 0.00121z^2}$$

where z = depth beneath ground surface in meters.

3.2.2 Evaluation of CRR

A plausible method for evaluating CRR is to retrieve and test undisturbed soil specimens in the laboratory. Unfortunately, in situ stress states generally cannot be reestablished in the laboratory, and samples of granular soils retrieved with typical drilling and sampling techniques are too disturbed to yield meaningful results. Only through specialized sampling techniques, such as ground freezing, can sufficiently undisturbed samples be obtained. The cost of such procedures is generally prohibitive for all but the most critical projects.

Several field tests have gained common usage for evaluation of liquefaction resistance, including the standard penetration test (SPT), the cone penetration test (CPT), shear wave velocity measurements (V_s), and the Becker penetration test (BPT).

3.2.2.1 SPT

Criteria for evaluating liquefaction resistance based on SPT are largely embodied in the CSR versus $N_{1(60)}$ plot shown in Figure 3-2. $N_{1(60)}$ is the SPT blow count normalized to an overburden pressure of approximately 100 kPa (1 ton/ft²) and a hammer energy ratio or hammer efficiency of 60%. Figure 3-2 is a plot of calculated CSR and corresponding

$N_{1(60)}$ data from sites where liquefaction effects were or were not observed following past earthquakes with magnitudes of approximately 7.5.

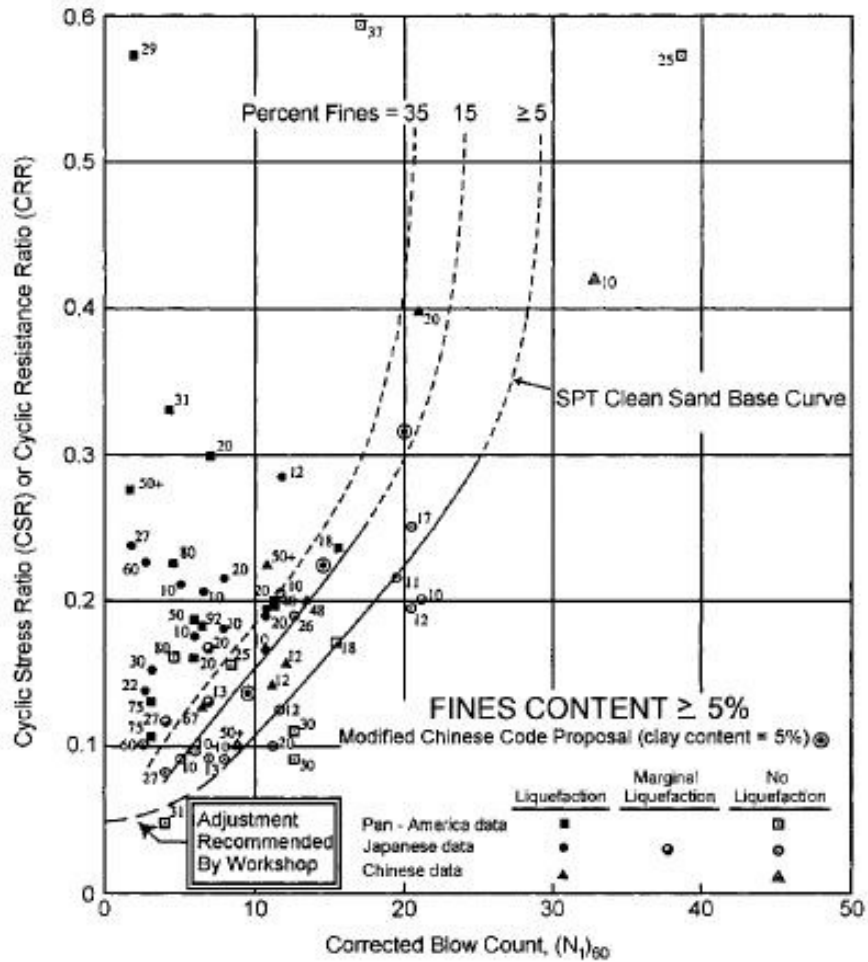


Figure 3-2: SPT Clean-sand base curve from magnitude 7.5 earthquakes with data from liquefaction case histories

Curves were developed for granular soils with the fines contents of 5% or less, 15% and 35% as shown on the plot. The CRR curve for fines less than 5% is the basic penetration criterion for the simplified procedure and is referred to as the “SPT clean-sand base curve”.

The clean-sand base curve that is plotted in Figure 3-2 may be approximated by the following equation (Youd et al. 2001):

$$CRR_{7.5} = \frac{1}{34 - (N_1)_{60}} + \frac{(N_1)_{60}}{135} + \frac{50}{[10 \cdot (N_1)_{60} + 45]^2} - \frac{1}{200}$$

This equation is valid for values of $N_{1(60)}$ that are less than 30. Where values of $N_{1(60)}$ are greater or equal than 30, the clean granular soils are too dense to liquefy and are classified as non-liquefiable.

In the original development of the method, an apparent increase of CRR with the increase of fines content was noted. Whether this increase was caused by an increase of liquefaction resistance or a decrease in penetration resistance is not clear. Seed and Idriss developed the following equations for correction of $N_{1(60)}$ to an equivalent $N_{1(60)cs}$:

$$N_{1(60)cs} = \alpha + \beta N_{1(60)}$$

where α and β are coefficients determined from the following relationships:

- $\alpha = 0$ for $FC \leq 5\%$
- $\alpha = \exp[1.76 - (190/FC^2)]$ for $5\% < FC < 35\%$
- $\alpha = 5$ for $FC \geq 35\%$
- $\beta = 1.0$ for $FC \leq 5\%$
- $\beta = [0.99 + (FC^{1.5}/1000)]$ for $5\% < FC < 35\%$
- $\beta = 1.2$ for $FC \geq 35\%$

These equations may be used for routine liquefaction resistance calculations.

Several factors in addition to fines content and grain characteristics influence SPT results as noted in Table 3-1.

Table 3-1: Corrections to standard penetration testing (after Youd et al. 2001)

Factor	Equipment variable	Term	Correction
Overburden pressure	—	C_N	$(P_a/\sigma'_{vo})^{0.5}$
Overburden pressure	—	C_N	$C_N \leq 1.7$
Energy ratio	Donut hammer	C_E	0.5–1.0
Energy ratio	Safety hammer	C_E	0.7–1.2
Energy ratio	Automatic-trip Donut-type hammer	C_E	0.8–1.3
Borehole diameter	65–115 mm	C_B	1.0
Borehole diameter	150 mm	C_B	1.05
Borehole diameter	200 mm	C_B	1.15
Rod length	<3 m	C_R	0.75
Rod length	3–4 m	C_R	0.8
Rod length	4–6 m	C_R	0.85
Rod length	6–10 m	C_R	0.95
Rod length	10–30 m	C_R	1.0
Sampling method	Standard sampler	C_S	1.0
Sampling method	Sampler without liners	C_S	1.1–1.3

The following equation is used to calculate these corrections:

$$N_{I(60)} = N_m C_N C_E C_B C_R C_S$$

where

- N_m = measured standard penetration resistance
- C_N = factor to normalize N_m to a common reference effective overburden stress
- C_E = correction for hammer energy ratio (ER)
- C_B = correction factor for borehole diameter
- C_R = correction factor for rod length
- C_S = correction for samplers with or without liners

Because SPT N-values increase with increasing effective overburden stress, an overburden stress correction factor should be applied (Seed and Idriss 1982). This factor is calculated from the following equation (Liao and Whitman 1986a):

$$C_N = \left(\frac{P_a}{\sigma'_{vo}} \right)^{0.5}$$

where C_N normalizes N_m to an effective overburden pressure σ'_{vo} of approximately 100 kPa (1 atm, P_a). C_N should not exceed a value of 1.7.

The effective overburden pressure σ'_{vo} applied in the equation above should be the overburden pressure at the time of drilling and testing. Although a higher ground water level can be used for conservatism in the liquefaction resistance calculations.

Another important factor is the energy transferred from the falling hammer to the Split spoon sampler. An ER of 60% is generally accepted as the approximate average for United States testing practice and as a reference value for energy corrections.

$$C_E = \frac{ER}{60}$$

The ER delivered to the sampler depends on the type of hammer, anvil, lifting mechanism, and the method of hammer release. Approximate correction factors to modify the SPT results to a 60% energy ratio for various types of hammers and anvils are listed in Table 3-1.

Skempton (1986) suggested and Robertson and Wride (1998) updated correction factors for rod lengths less than 10 m, borehole diameters outside the recommended interval (65-125 mm), and sampling tubes without liners. These correction factors are listed in Table 3-1.

3.2.2.2 CPT

Robertson and Wride (1998), and reported by Youd et al. (2001) prepared curves for direct determination of CRR for clean sands ($FC \leq 5\%$) from CPT data. The curves were developed from CPT case history data compiled from several investigations, including those by Stark and Olson (1995) and Suzuki et al. (1995). The original curve can be seen plotted in Figure 3-3.

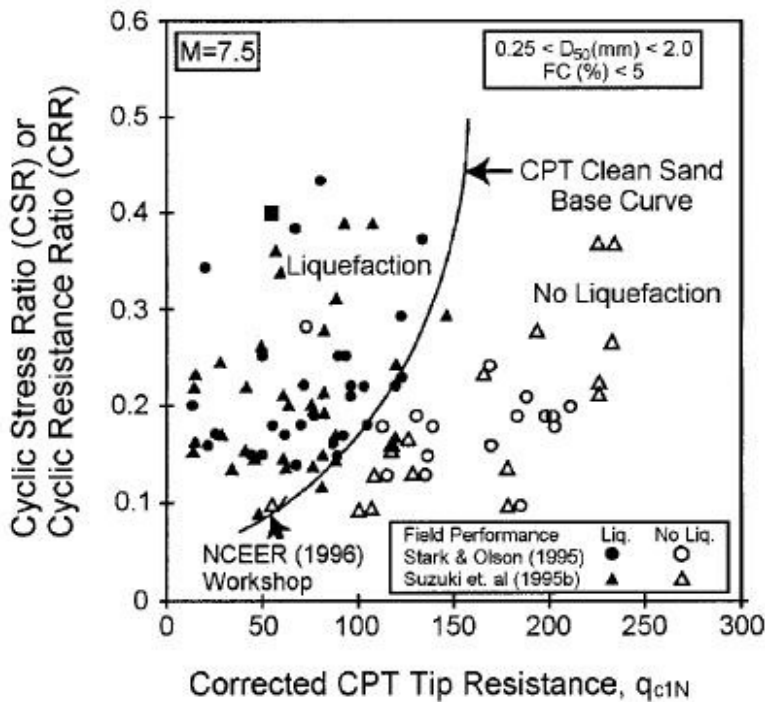


Figure 3-3: Curve recommended for calculation of CRR from CPT data along with empirical liquefaction data from compiled case histories (after Youd et al. 2001).

The clean sand base curve in Figure 3-3 may be approximated by the following equation (Robertson and Wride 1998):

$$\text{If } (q_{c1N})_{cs} < 50, \text{ then } CRR_{7.5} = 0.833 \left[\frac{(q_{c1N})_{cs}}{1000} \right] + 0.05$$

$$\text{If } 50 \leq (q_{c1N})_{cs} < 160, \text{ then } CRR_{7.5} = 93 \left[\frac{(q_{c1N})_{cs}}{1000} \right]^3 + 0.08$$

where $(q_{c1N})_{cs}$ is the clean sand cone penetration resistance normalized to approximately 100 kPa (1 atm).

The CPT procedure requires normalization of tip resistance. This transformation yields normalized, dimensionless cone penetration resistance q_{c1N} .

$$q_{c1N} = C_Q (q_c / P_a)$$

and

$$C_Q = (P_a / \sigma'_{vo})^n$$

where:

C_Q = normalizing factor for cone penetration resistance

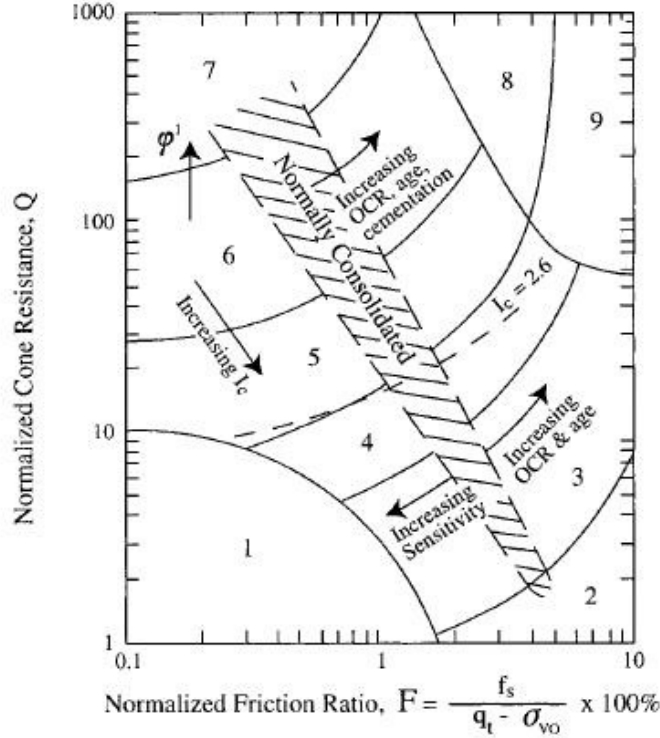
P_a = 1 atm of pressure in the same units used for σ'_{vo}

n = exponent that varies with soil type

q_c = field cone penetration resistance measured at the tip

At shallow depths C_Q becomes large because of low overburden pressure and values greater than 1.7 should not be applied. The value of the exponent n varies from 0.5 to 1.0, depending on the grain characteristics of the soil (Youd et al. 2001).

The CPT friction ratio (sleeve resistance f_s divided by cone tip resistance q_c) generally increases with increasing fines content and soil plasticity, allowing rough estimates of soil type and fines content to be determined from CPT data. Robertson and Wride (1998) constructed a chart reproduced in Figure 3-4 for estimation of soil type.



- | | |
|--|-------------------------------------|
| 1. Sensitive, fine grained | 6. Sands - clean sand to silty sand |
| 2. Organic soils - peats | 7. Gravelly sand to dense sand |
| 3. Clays - silty clay to clay | 8. Very stiff sand to clayey sand* |
| 4. Silt mixtures - clayey silt to silty clay | 9. Very stiff, fine grained* |
| 5. Sand mixtures - silty sand to sandy silt | |
- *Heavily overconsolidated or cemented

Figure 3-4: CPT-based soil behavior type chart proposed by Robertson (1990)

The radius of the circles shown in Figure 3-4, termed the soil behavior type index I_c is calculated from the following equation:

$$I_c = \left[(3.47 - \log Q)^2 + (1.22 + \log F)^2 \right]^{0.5}$$

where

$$Q = \left(\frac{q_c - \sigma_{vo}}{P_a} \right) \left(\frac{P_a}{\sigma'_{vo}} \right)^n$$

and

$$F = \left(\frac{f_s}{q_c - \sigma_{vo}} \right) \times 100\%$$

The soil behavior chart in Figure 3-4 was developed using an exponent n of 1.0, which is the appropriate value for clayey soil types. For clean sands, however, an exponent value of 0.5 is more appropriate, and a value between 0.5 and 1.0 would be appropriate for silts and sandy silts.

Robertson and Wride recommended the following procedure for calculating the soil behavior type index I_c . The first step is to differentiate soil types characterized as clays from soil types characterized as sands and silts. This differentiation is performed by assuming an exponent n of 1.0 and calculating the dimensionless CPT tip resistance Q from the following equation:

$$Q = \left(\frac{q_c - \sigma_{vo}}{P_a} \right) \left(\frac{P_a}{\sigma'_{vo}} \right)^{1.0} = \frac{q_c - \sigma_{vo}}{\sigma'_{vo}}$$

If the I_c calculated with an exponent of 1.0 is greater than 2.6, the soil is classified as clayey and is considered too clay-rich to liquefy, and the analysis is complete. However, soil samples should be retrieved and tested to confirm the soil type and liquefaction resistance. Criteria such as the Chinese criteria might be applied to confirm that the soil is non-liquefiable. The so-called Chinese criteria, as defined by Seed and Idriss (1982), specify that liquefaction can only occur if all three of the following conditions are met:

- The clay content (particles smaller than 5 μ) is less than 15% by weight.
- The liquid limit is less than 35%.
- The natural moisture content is greater than 0.9 times the liquid limit.

If the calculated I_c is less than 2.6, the soil is most likely granular in nature, and therefore C_Q and Q should be recalculated using an exponent n of 0.5. I_c should then be recalculated. If the recalculated I_c is less than 2.6, the soil is classified as non-plastic and granular and this I_c should be used to estimate the liquefaction resistance. However, if the recalculated I_c is greater than 2.6, the soil is likely to be very silty and possibly plastic. In this case, q_{c1N} should be recalculated using an intermediate exponent n of 0.7. I_c is then recalculated once again. This intermediate I_c is the used to calculate liquefaction resistance. In this instance, a soil sample should be retrieved and tested to verify the soil type and whether the soil is liquefiable by other criteria such as the Chinese criteria.

The normalized penetration resistance (q_{c1N}) for silty sands is corrected to an equivalent clean sand value $(q_{c1N})_{cs}$, by the following relationship:

$$(q_{c1N})_{cs} = K_c q_{c1N}$$

where K_c , the correction factor for grain characteristics, is defined by the following equation (Robertson and Wride 1998):

for $I_c \leq 1.64$, $K_c = 1.0$; and

$$\text{for } I_c > 1.64, K_c = -0.403I_c^4 + 5.581I_c^3 - 21.63I_c^2 + 33.75I_c - 17.88$$

With an appropriate I_c and K_c values, the equations above can be used to calculate $CRR_{7.5}$.

3.3 Magnitude Scaling Factors (MSFs)

The clean sand base or CRR curves plotted before, apply only to magnitude 7.5 earthquakes. To adjust these curves to magnitudes smaller or larger than 7.5, Seed and Idriss (1982) introduced correction factors termed “magnitude scaling factors (MSFs)”. These factors are used to scale the CRR base curves upward or downward on CRR versus $N_{1(60)}$ or $(qc_1)_N$ plots.

To illustrate the influence of magnitude scaling factors on calculated hazard, the equation for factor of safety (FS) against liquefaction is written in terms of CRR, CSR, and MSF as follows:

$$FS = \left(\frac{CRR_{7.5}}{CSR} \right) MSF$$

where:

- CSR = calculated cyclic stress ratio generated by the earthquake shaking
- $CRR_{7.5}$ = cyclic resistance ratio for magnitude 7.5 earthquakes

The MSFs can be calculated using Seed’s revised equation as follows:

$$MSF = \frac{10^{2.24}}{M_w^{2.56}}$$

This equation reduces the CRR if the magnitude of the earthquake is greater than 7.5, and increases it if it is less than 7.5.

CHAPTER 4: CASE HISTORIES OF LIQUEFACTION

4.1 Liquefaction evaluation based on CPT and SPT Data

All of the liquefaction evaluation analyses performed in this study were made using the simplified procedure proposed by Seed and Idriss (1971) and revised by Youd et al. (2001); details of the procedure were explained in Chapter 3. For ease of interpreting the results, the factor of safety versus depth was evaluated and plotted. Based on physical evidence recovered during a post-earthquake reconnaissance (Bray et al. (2001), all three of the sites investigated showed evidence of liquefaction during the earthquake. The results of this evaluation show the critical layers at which liquefaction was likely to have initiated. The calculations and pertinent information are presented in Appendix ##.

4.2 South Seattle Site

4.2.1 Site Description

Evidence of liquefaction was observed over a large area in the industrial “Sodo” district of Seattle, which is located south of downtown. One site of interest within this area, located between First Avenue South and Occidental Street, is shown in Figure 4-1. Of particular interest is the building located at 2910 1st Avenue South), which is the

second of four buildings in a row from north to south. Each of these buildings appeared to be both similar vintage and construction type.

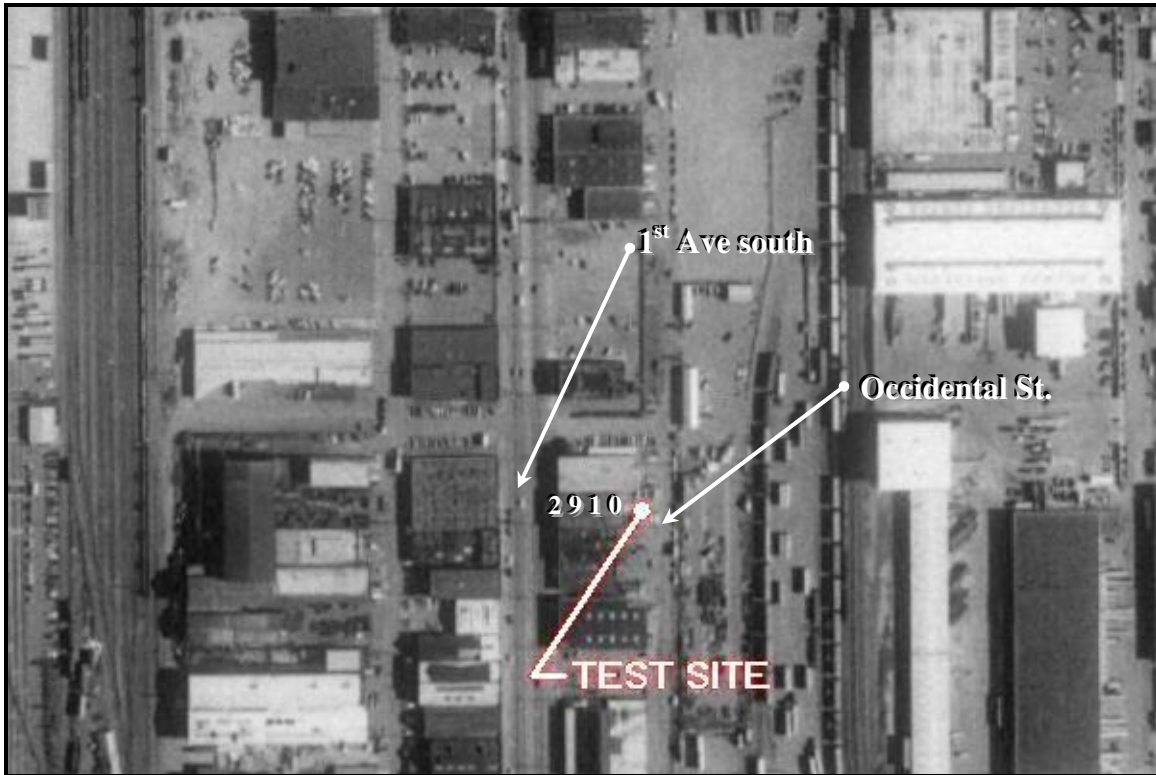


Figure 4-1: Aerial picture showing the location of 2910 First Avenue South.

4.2.2 Observations of earthquake effects

Within this zone, structural performance varied greatly from building to building. The buildings did vary in age, type of construction, and foundation details, which were likely factors in the observed performance. However, it is evident that other factors such as subsurface soil conditions were also important. Like many urban areas that experience extensive liquefaction during seismic events, the Sodo area was developed using hydraulic fill – fill soils that were transported and deposited as a suspension in water without significant additional densification or other activities (e.g., compaction or vibration) that would tend to enhance their seismic performance.

Of particular interest is an industrial block along First Avenue South where structural performance varied from catastrophic collapse to moderate damage to essentially no damage as shown in Figure 4-2. Building 3 in the moderate damage area of this block was our case study. In this particular building, seven sand boils were found in the crawl space below the first floor, making it clear that liquefaction had occurred in the subsurface soils. Samples of ejecta were collected from these sand boils. These ejecta samples showed a substantial fraction of non-plastic fines (5 to 20 percent passing the #200 sieve). The large amount of silt recovered within the ejecta indicates that there was likely silty sand underlying the site.



Figure 4-2: Four adjacent unreinforced masonry buildings along 1st Avenue South. Each of the buildings experienced increasing damage from right to left. Building 3 was the primary site of interest at 2910 S. First Avenue South.

4.2.3 Subsurface Soil Conditions and Liquefaction Evaluation

Four CPT borings were performed on the south Seattle site. The location of these borings with respect to the four buildings of interest is shown in Figure 4-3. The global positioning system (GPS) coordinates for these borings are shown in Table 4-1.

Subsurface soil conditions along this block are shown by the profile in Figure 4-4. Ground water level was found at approximately 9 feet. Directly under building 3, CPT-67 shows that the upper 3 to 5 feet of soils encountered were poorly graded clean sands that appear to be from the early 1900's regrading of Seattle. These sands had no more than 7% fines (passing the No. 200 sieve). The higher tip resistances of these soils may have been caused by the change in depth of the water table, which fluctuates seasonally. This causes jetting in the top layer of soil increasing the bearing capacity of it. The same types of soils were found under CPT-70 located about 120 feet south of the building. From 5 to 13 feet of depth we found again poorly graded clean sands with a lower tip resistance. From 13 to around 17 feet a small layer of finer grained material was found. This layer had an increasingly amount of fines ranging from 15 up to 51% fines. It had also the lowest tip resistances and the lowest SPT blow counts. It is very important to notice that this layer was not encountered under CPT-70. Some research studies have found that liquefaction may actually be a form of base isolation during seismic events. This may have been one of the reasons why the two buildings under the softer layer suffered less structural damage. Clean sands with some silty lenses lie under this layer up to 40 feet deep. Their tip resistance now increases gradually until bay clay is found at a depth of 40 feet

Table 4-1: GPS coordinates of CPT borings for the South Seattle site.

Boring No.	Position	
	Latitude	Longitude
CPT - 67	N 47 34.640	W 122 20.008
CPT - 68	N 47 34.641	W 122 20.007
CPT - 69	N 47 34.647	W 122 20.008
CPT - 70	N 47 34.622	W 122 20.000

* Formats: Lat/Lon ddd° mm.mmm'

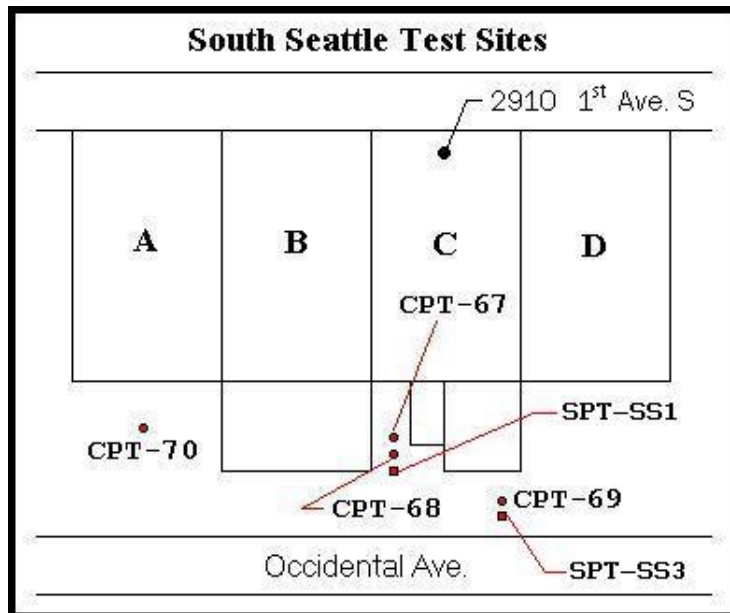


Figure 4-3: Location of CPT and SPT borings on the south Seattle site.

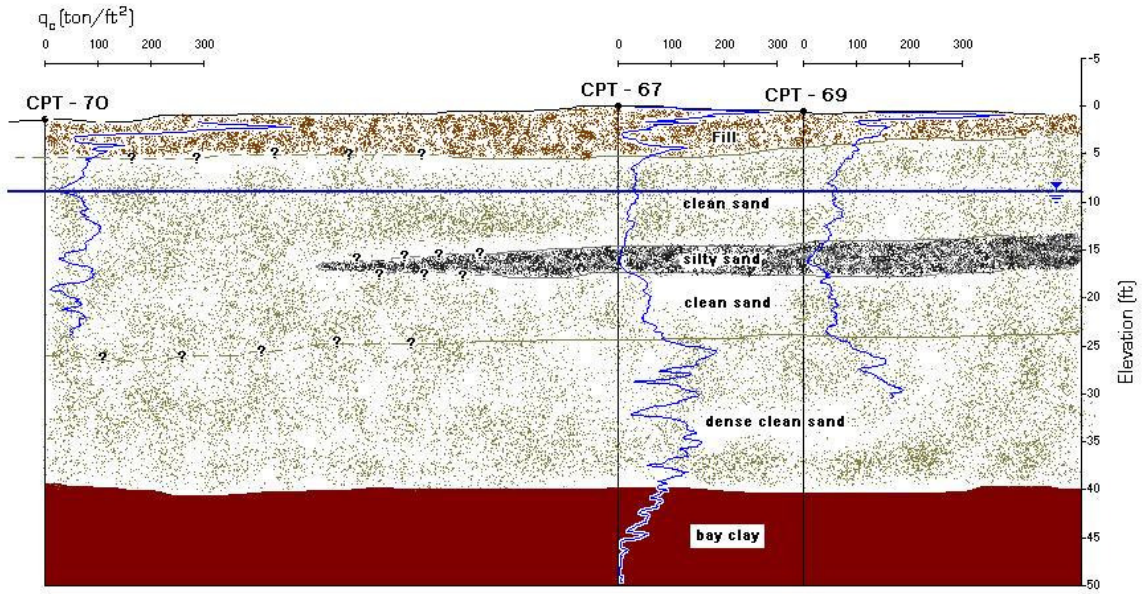


Figure 4-4: Subsurface cross-section at south Seattle based on CPT profiling. Shown are the tip resistances at their relative locations for the three CPT profiles completed.

Each of the CPT profiles is presented separately. The profile for CPT-67 is shown in Figure 4-5.

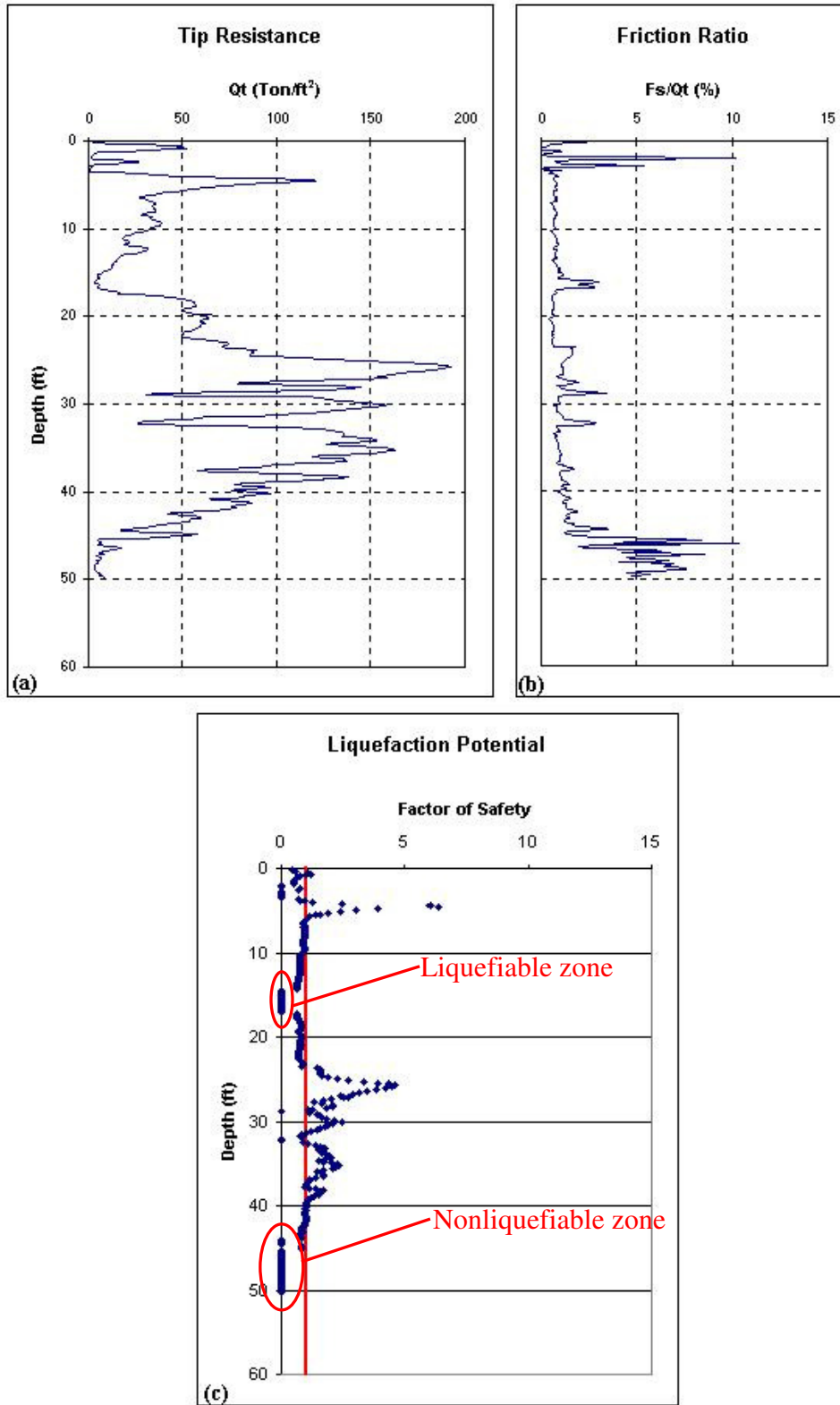


Figure 4-5: CPT-67 used in liquefaction evaluation. (a) Tip resistance. (b) Friction ratio. (c) Liquefaction potential.

For the profile shown in Figure 4-5(c), the critical liquefiable layer was found at a depth from about 14 feet to 17 feet. This does not mean that this is the only layer that liquefied; just that it appears to be the most vulnerable. Overall, the liquefiable material for this profile may involve all of the soil from a depth as shallow as 7 feet to a depth of 24 feet. However, at the time the profile was made, the depth to the water table was at a depth of 9 feet. As the depth to the water table at the time of the earthquake is unknown, some uncertainty about the liquefaction potential of the upper soils is evident.

Figure 4-5(c) also shows that at a depth of 14 feet to 17 feet, the factor of safety against liquefaction approaches 0. Given this result, it indicates that the soil may contain sufficient fines such that the Chinese criteria should now then be evaluated. This criteria evaluates the clay content of the fines to determine the liquefaction potential. Hydrometer tests were performed on soil samples recovered from this layer (depth of 14 feet to 17 feet). The results indicate that the clay content was less than 15%, which indicates that although the soil contained a large percentage of fines, they were silty and nonplastic. In this site, the highest clay content was found to be about 1.2% at a depth of about 16 feet. Although the liquid limit was determined to be a little less than 35%, the plastic limit was undefined (the soil would not roll in threads) and hence, the soil is nonplastic. Since the soils were nonplastic, the Chinese criteria for liquefaction were satisfied and hence, the layer can be classified as liquefiable.

Figure 4-5(c) also shows that the factor of safety against liquefaction approaches 0 at a depth of about 45 feet. Because it was assumed that the overburden stresses at these depths were too high to allow liquefaction, no soil samples were recovered from this depth. Additionally, as seen in Figure 4-5(b), the average friction ratio at this depth is about 2.5 times the friction ratio of the layer discussed previously. Based on this, these soils are likely bay clays that should possess sufficient clay fines (and hence, plasticity) such that the Chinese criteria would have not been met. Therefore, this layer was considered to be nonliquefiable.

CPT-68 will not be shown since this boring was made only to verify that the cone penetrometer was working properly.

CPT-69, completed about 30 feet north of CPT-67, is presented in Figure 4-6. This profile is very similar to that from CPT-67 but the silty layer in that profile (depth 14 feet to 17 feet) appears to be thinner indicating that the thickness of the layer diminishes toward the north. Figure 4-6(c) shows the factor of safety versus depth from the profile at CPT-69.

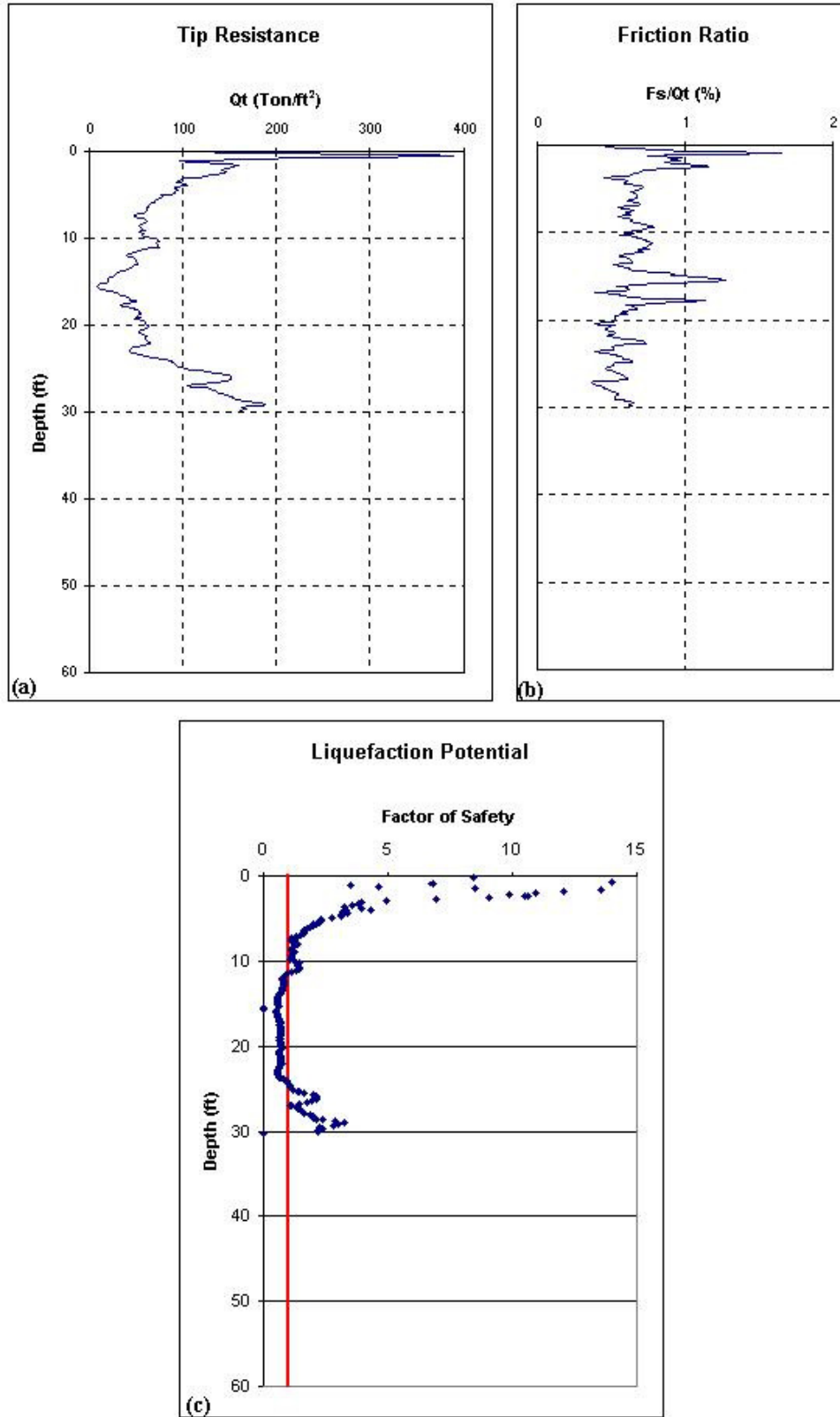


Figure 4-6: CPT-69 used in liquefaction evaluation. (a) Tip resistance. (b) Friction ratio. (c) Liquefaction potential.

The results indicate that the total thickness of the liquefiable layer at this profile has decreased from 17 feet (-7 feet to -24 feet) to a thickness of only 12 feet (-12 feet to -24 feet). It is also shown that number of data points where the factor of safety approaches 0 is reduced to just two points (17.55 to 17.72 feet deep). This indicates that the thickness of the silty liquefiable material, as determined by the Chinese criteria, decreases toward the north.

CPT-70 was located about 130 feet south of the other two borings. The soil profile for this boring can be seen in figure 4-7. It can be seen in figure 4-7(c) that in this boring, the liquefiable zone has greatly decreased from a thickness of about 17 feet to just two small layers of about 1 foot thick. The first layer shows at a depth of about 7 feet, while the second layer is at a depth of about 15 feet. It is believed that since this boring is less susceptible to liquefaction more seismic energy might have been transferred to the south of the block. This stiffness allows more motion (vertically propagating shear waves) to get up to the surface. The buildings to the north had a much thicker layer of liquefiable zone. It is known that liquids don't transmit shear waves hence making the liquefied zone less vulnerable to seismic shear waves. This may be one of the reasons of why buildings to the south of the site performed poorly during the earthquake.

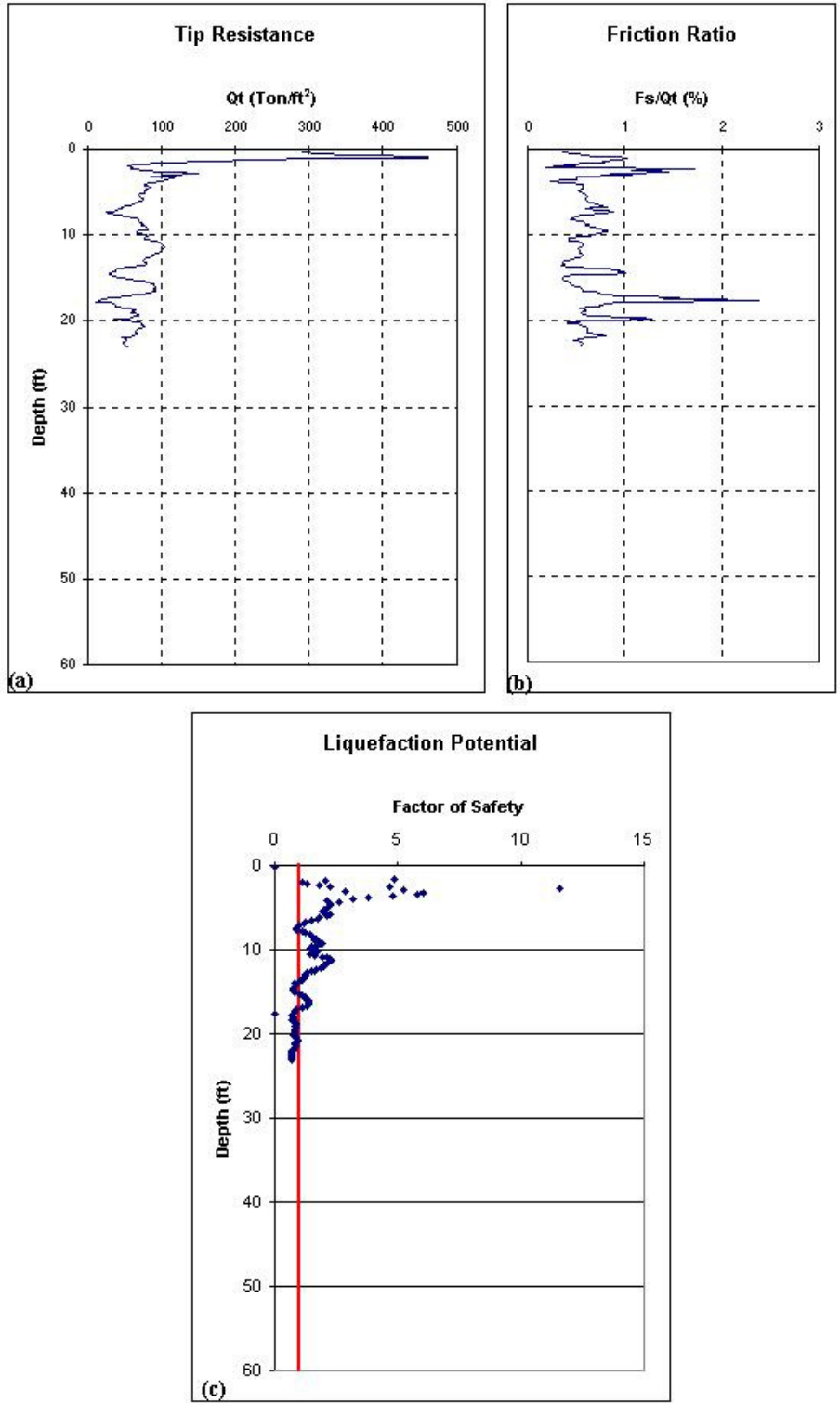


Figure 4-7: CPT-70 used in liquefaction evaluation. (a) Tip resistance, (b) Friction ratio, and (c) Liquefaction potential.

SPT blow counts were also used to conduct liquefaction evaluation analyses. For the south Seattle site only two borings were drilled using Standard penetration tests. The other two borings were sampled using Shelby tubes. The results for the liquefaction analysis on the first boring in the south Seattle site (SS1) can be seen in Figure 4-8. Boring SS1 was located only 5 feet east of the location of CPT-67. This allowed correlating the SPT results to the CPT results. Figure 4-8 consists of a table showing the results of the liquefaction analysis and a plot showing the liquefaction potential of the site.

Hammer Type	Depth (Z) (ft)	N	r_a	σ_{vo} (psf)	σ'_{vo} (psf)	CSR	$(N_1)_{60}$	FS
Auto	3	6	0.979	364.17	364.17	0.153	16	1.438
Auto	4.5	5	0.969	541.34	541.34	0.151	11	1.024
Cathead	6	7	0.958	718.51	718.51	0.149	9	0.879
Cathead	7.5	12	0.943	895.67	839.37	0.157	10	0.911
Cathead	9	7	0.923	1072.84	924.41	0.167	7	0.652
Cathead	11	6	0.883	1328.74	1047.25	0.175	7	0.624
Auto	13.5	2	0.811	1624.02	1188.98	0.173	4	0.458
Auto	18.5	5	0.654	2214.57	1472.44	0.153	10	0.931
Auto	21	7	0.598	2529.53	1623.63	0.145	14	1.325
Auto	23.5	12	0.559	2824.81	1765.36	0.140	21	2.139
Auto	26	6	0.532	3120.08	1907.09	0.136	10	1.053

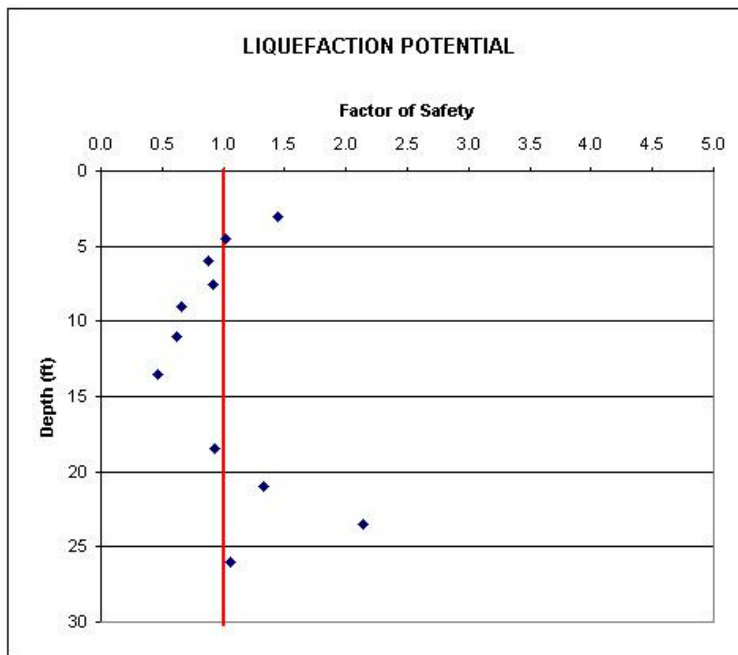


Figure 4-8: Results of SPT liquefaction analysis for boring SS1.

The SPT results for South Seattle 1 (SPT-SS1) shows a perfect correlation with the results obtained for CPT-67, which was only 5 feet away. The liquefiable layer is shown to be from a depth of about 4 feet to a depth of about 18 feet. Both the SPT and CPT analysis for this site show significant similarities in the liquefiable zone. Once again, the critical layer or most susceptible to liquefaction appears to be from about a depth of 14 feet to about a depth of 17 feet. These correlations are very interesting since both

exploration methods, SPT and CPT, may be used to produce adequate liquefaction evaluations. These evaluations should be accompanied with appropriate soil samples to confirm soil classification and property analysis.

Figure 4-9 shows the results for SPT-SS3. This boring was made just 5 feet east of CPT-69. This allows for correlation of the results. These results show a liquefiable layer that begins at about a depth of 7 feet. The end of this layer could not be determined since this was the end of the boring. Yet, the liquefiable layer seems to have decreased or at least the starting point has gone lower. These results also correlate perfectly with the CPT-69 results. Once again showing that the two methods can be expected to yield similar results.

Hammer Type	Depth (Z) (ft)	N	r_f	σ_{vo} (psf)	σ'_{vo} (psf)	CSR	$(N_1)_{60}$	FS
Auto	3.5	11	0.976	420.00	420.00	0.152	29	3.335
Auto	6	6	0.958	720.00	720.00	0.149	16	1.469
Auto	8.5	4	0.93	1020.00	899.05	0.165	10	0.868
Auto	11	5	0.883	1320.00	1043.05	0.174	11	0.888
Auto	13.5	4	0.811	1620.00	1187.05	0.173	8	0.695

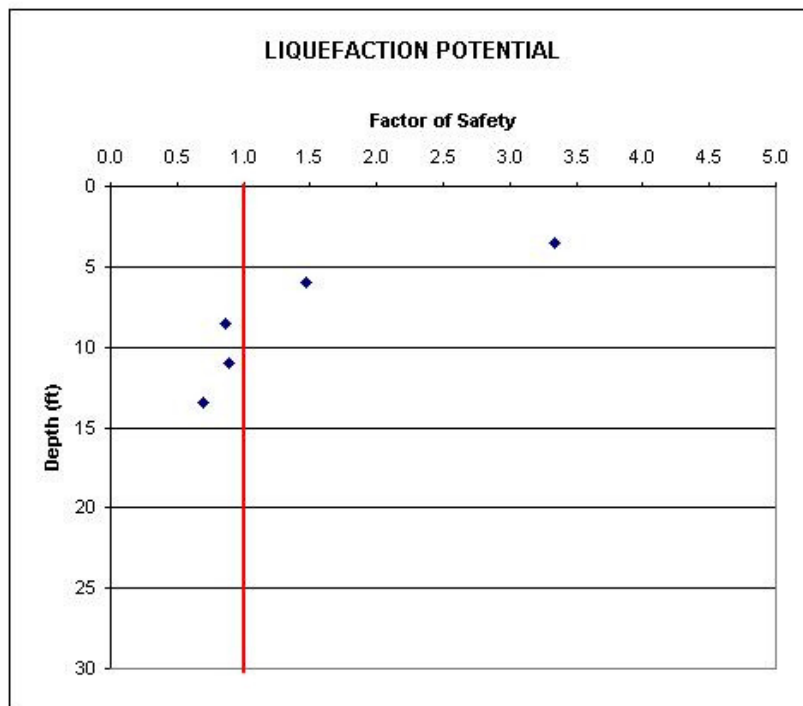


Figure 4-9: Results of SPT liquefaction analysis for boring SS3.

4.3 Port of Olympia

4.3.1 Site Description

The Port of Olympia is a municipal corporation serving for the Thurston County Port District. It also serves as a community port for recreation. Figure 4-10 shows a map of the location of the site. This port has been expanding throughout the years into the bay. The part investigated was built using hydraulic fill.

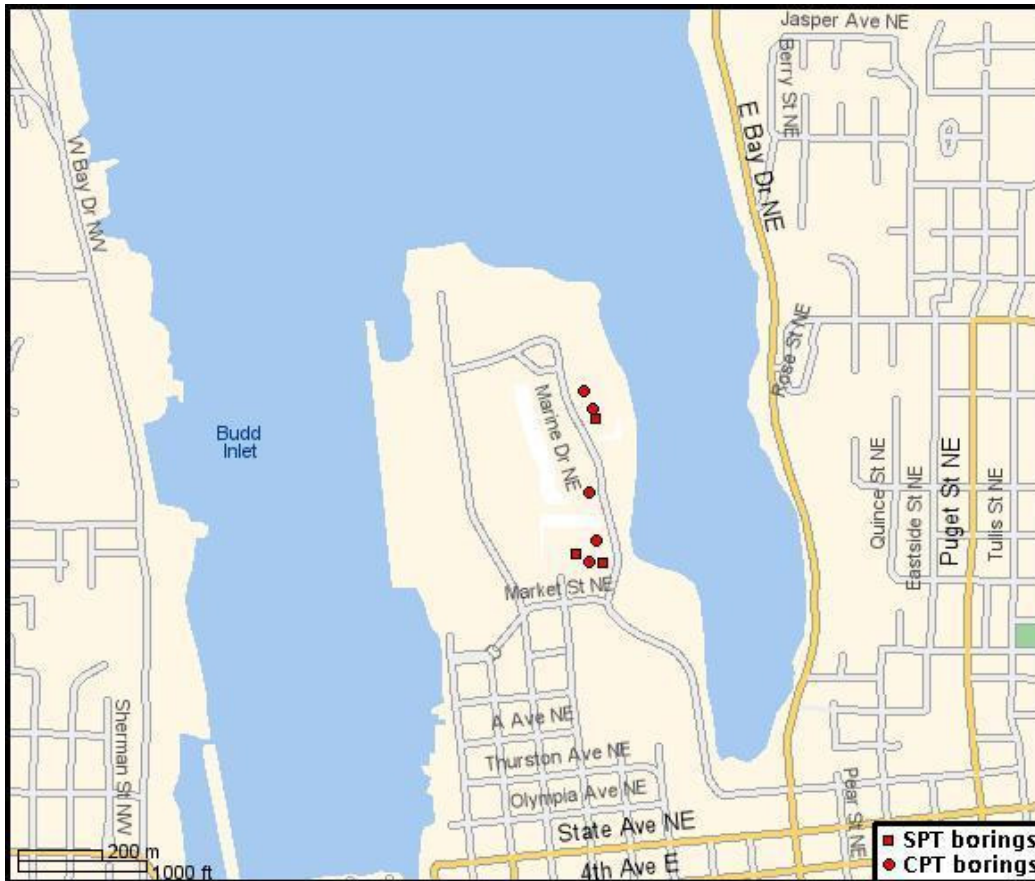


Figure 4-10: Location map of Port of Olympia test site.

4.3.2 Observations of Earthquake Effects

Several cases of lateral spreading, settlement and sand boils were found in the surroundings of the Port of Olympia (the Port). The land investigated was hydraulic fill placed to expand the ports capacity and function not only as a commercial port but also as a recreational area for a new marina. After the earthquake, several of the roads across this man made port were severely cracked indicating a case of lateral spreading or settlement. Figure 4-11 shows some of the cracks developed in the roads inside the Port.



Figure 4-11: Cracks developed at the Port of Olympia.

4.3.3 Subsurface soil conditions and Liquefaction Evaluation

A section of the subsurface soil conditions at the Port of Olympia are shown by the profile in Figure 4-12.

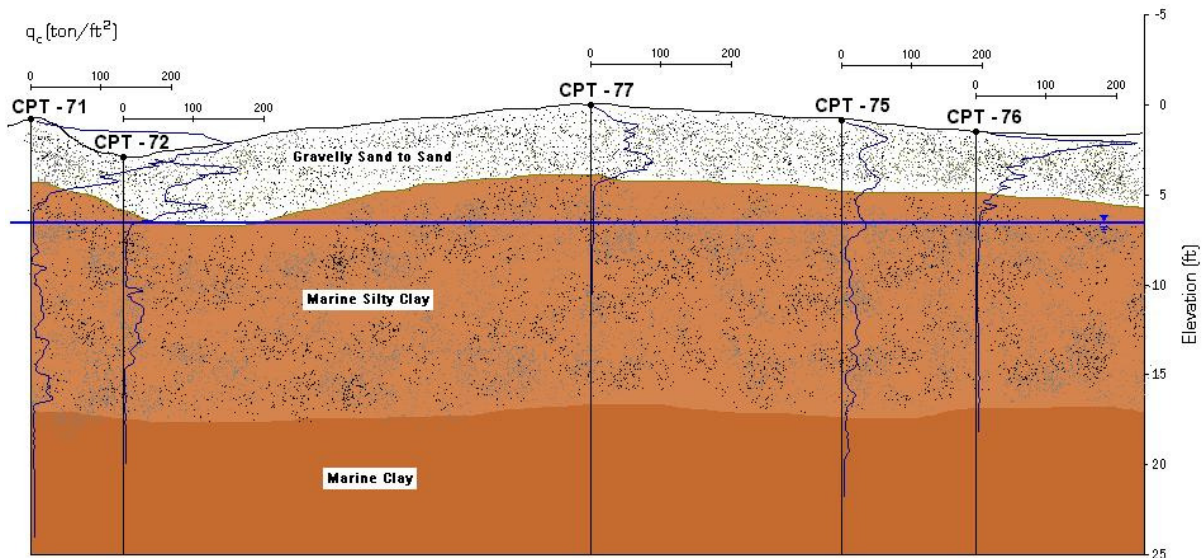


Figure 4-12. Subsurface cross-section at the Port of Olympia

The ground water level was found to be at 7 feet. Because it is located right next to the bay, the water level can change with the tides. As seen in the picture it is clear that the first five feet is the hydraulic fill placed over the bay to expand the size of the port. Under these five feet a silty clayey layer is found with some interchangeable layers of

sandy material. This sandy or silty material may have been the result of the finer material invading the top layers after the hydraulic fill was placed. This layer turned out to be around 10 feet thick. Under the silty clay, a layer of marine clay was found. The depth of this layer was not discovered since it is known that these clay layers do not liquefy and there was no reason for the borings to go any deeper.

The CPT liquefaction evaluations for this site are presented below. Each boring is presented and explained separately. A map showing the location of these borings was shown in Figure 4-10. The GPS coordinates can be found on Table 4-2.

Table 4-2: GPS coordinates of CPT borings for the Port of Olympia site.

Boring No.	Position	
	<i>Latitude</i>	<i>Longitude</i>
CPT - 71	N 47 03.314	W 122 53.970
CPT - 72	N 47 03.295	W 122 53.959
CPT - 75	N 47 03.146	W 122 53.903
CPT - 76	N 47 03.118	W 122 53.917
CPT - 77	N 47 03.196	W 122 53.934

* Formats: Lat/Lon ddd° mm.mmm'

Figure 4-13 shows the results for CPT-71. In this first boring a liquefiable layer appears from a depth of about 5 feet and continues down until the end of the boring. Unluckily no soil samples were recovered from the Standard penetration tests at this site. Shelby tubes were sampled and analyzed. The Shelby tubes started at a depth of 3 feet and all of them turned out to be marine clay. This indicates that the fine content of the soils encountered at the Port of Olympia are too clay rich to liquefy. From ten to fifteen feet, alternating layers of sandy material appear. These may have been small liquefiable layers. Since the soil samples recovered from this site did not show these layers no definite conclusion can be made of the site.

Figure 4-14 shows the liquefaction analysis for CPT-72. This profile shows similarity with CPT-71. These two borings were separated about 120 feet. The profile shows again a small layer of sandy material at about a depth from 7 feet to 12 feet. Once again, this layer is the most probable to have liquefied. This layer was also found on CPT-71. Both layers had a factor of safety either close to one or less than one. At this north part of the site is where more evidence of liquefaction was found. This indicates that some type of liquefaction must have occurred in these small sandy layers.

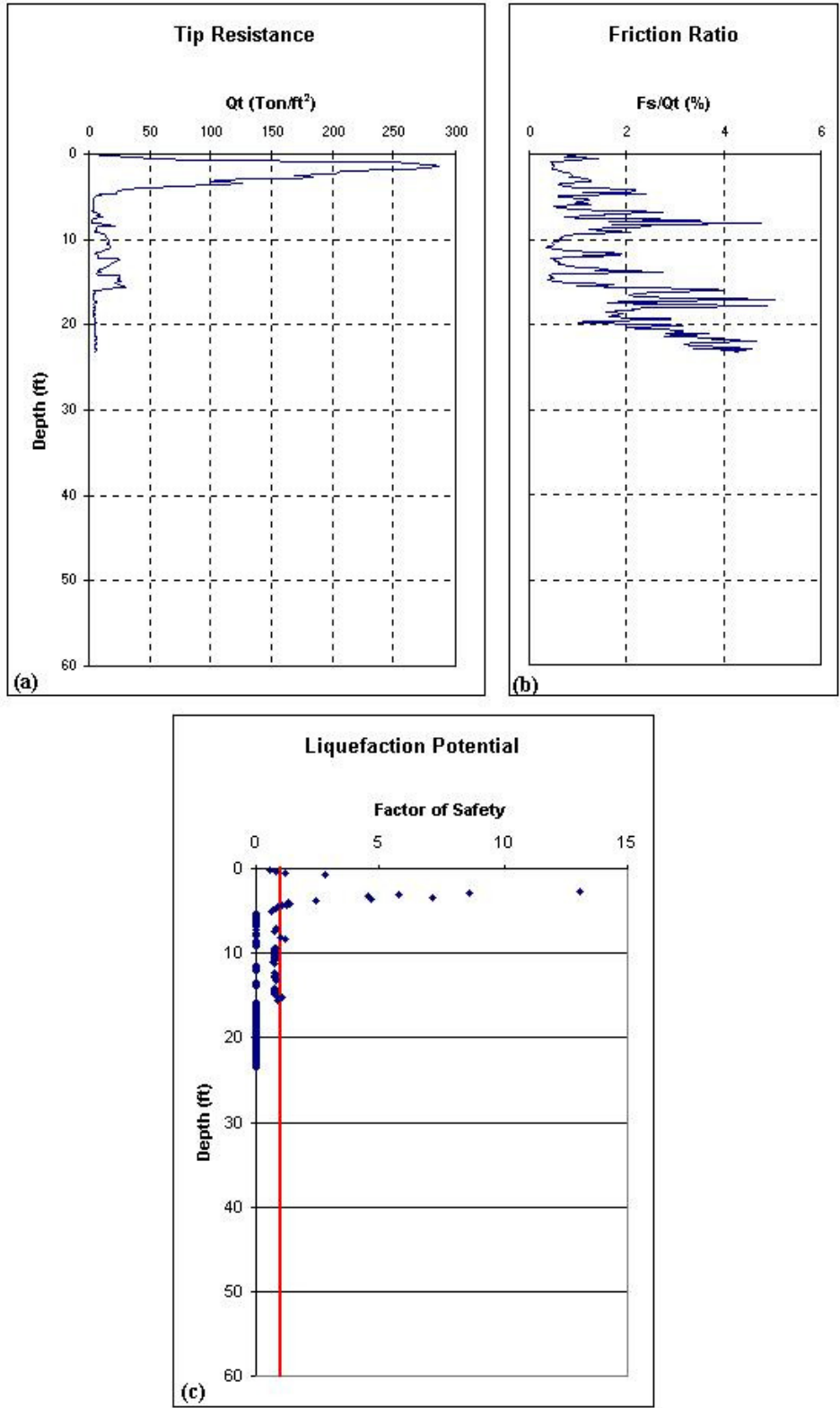


Figure 4-13: CPT-71 used in liquefaction evaluation. (a) Tip resistance, (b) Friction ratio, and (c) Liquefaction potential.

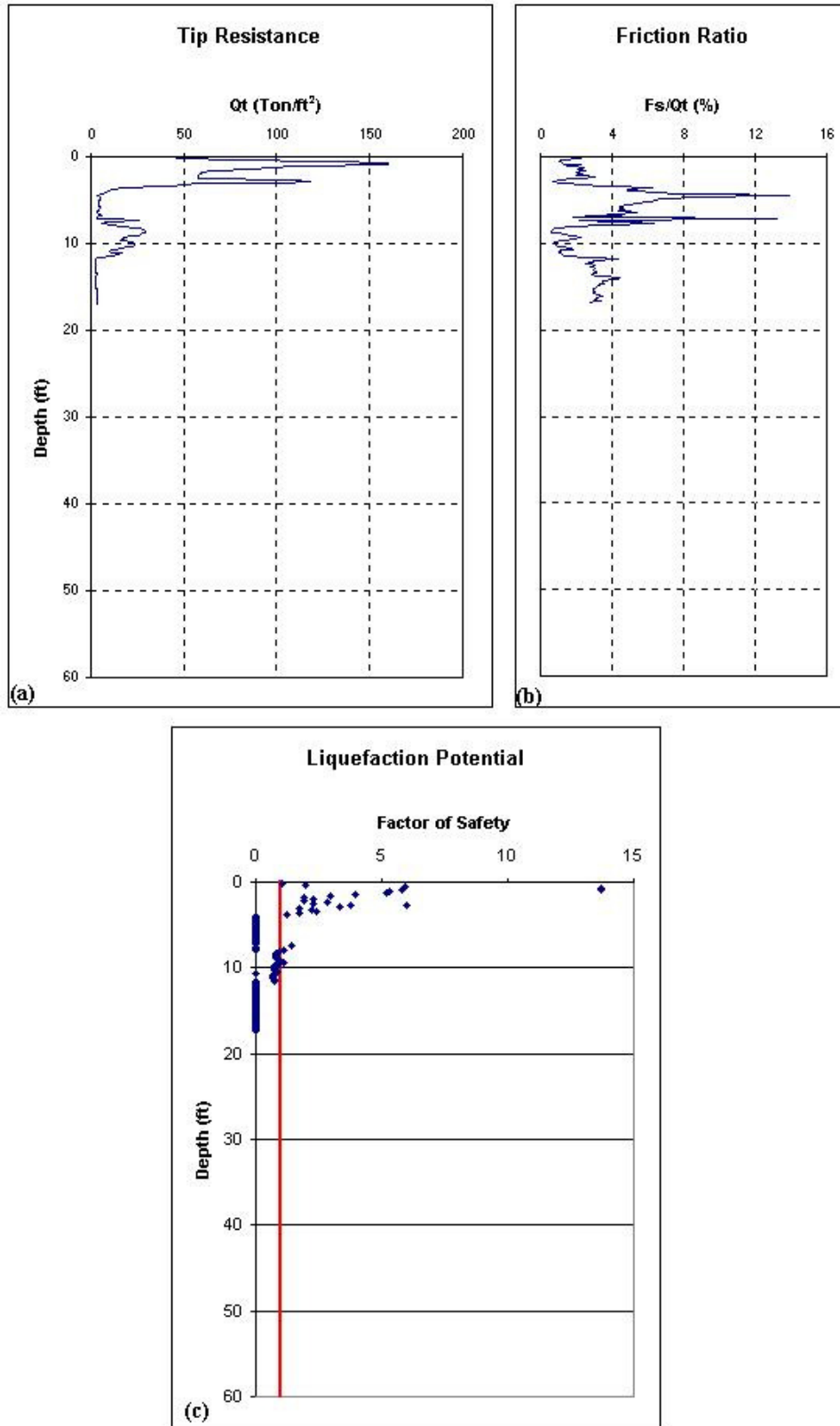


Figure 4-14: CPT-72 used in liquefaction evaluation. (a) Tip resistance, (b) Friction ratio, and (c) Liquefaction potential.

Figure 4-15 shows the results for CPT-75. The results are similar to those discussed previously for CPT-71 and CPT-72. The liquefiable layer appears to start from the surface, although in order to have liquefaction the layer needs to be under the water table. This eliminates the first 7 feet of the profile to the liquefaction susceptibility. This statement is only true if the water table remains at the same level at all times. The water table may vary affecting the liquefaction potential of some layers.

Results for CPT-76 can be seen in Figure 4-16. In this profile the liquefiable layer appears from about 4 feet until the end of the boring. This layer is definitely not liquefiable. No sandy material was found after 5 feet. This part of the site did not show evidence of liquefaction. Though the factor of safety for this profile shows zero after five feet, this only indicates that the soil is too clay rich to liquefy.

Figure 4-17 shows the results for CPT-77. This profile was only taken down to 10 feet. It shows the same characteristics as CPT-76. These last three profiles (CPT-75, CPT-76, and CPT-77) were around the same location while the first two profiles were located a little more to the north. The north part of the site appears to be sandier than the south part of it. This makes liquefaction potential higher in the north side than in the south side of this part of the Port of Olympia.

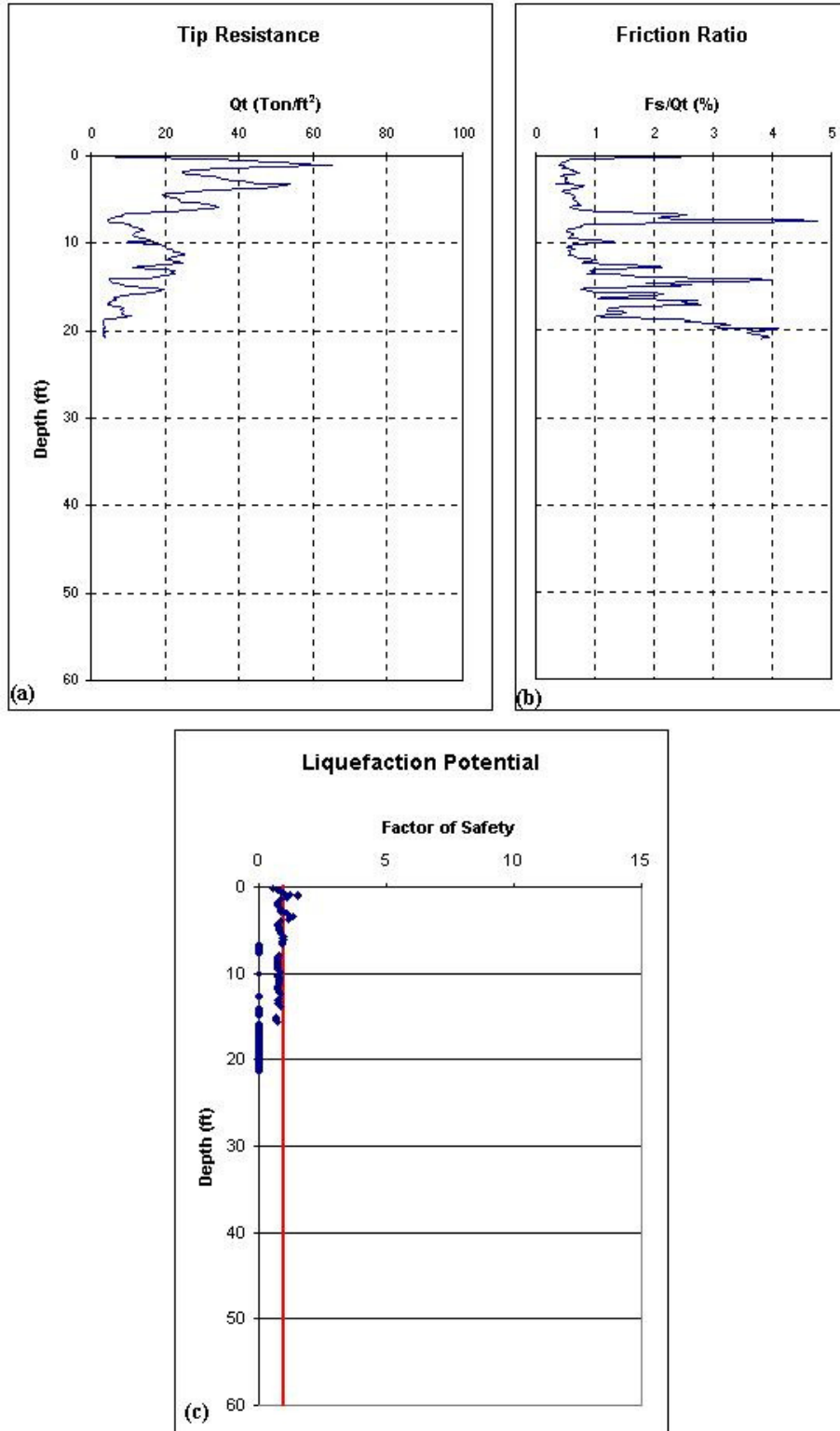


Figure 4-15: CPT-75 used in liquefaction evaluation. (a) Tip resistance, (b) Friction ratio, and (c) Liquefaction potential.

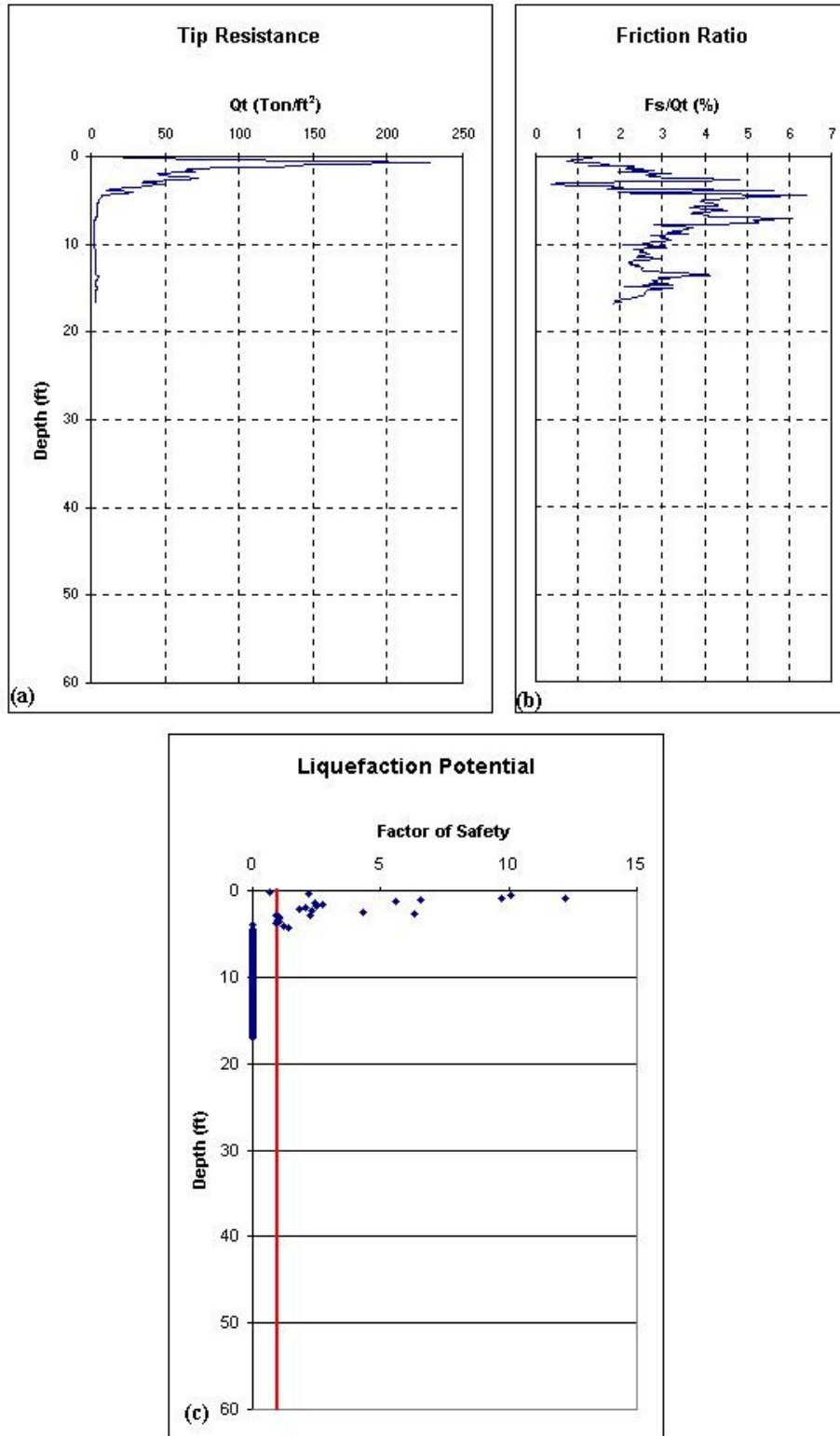


Figure 4-16: CPT-76 used in liquefaction evaluation. (a) Tip resistance, (b) Friction ratio, and (c) Liquefaction potential.

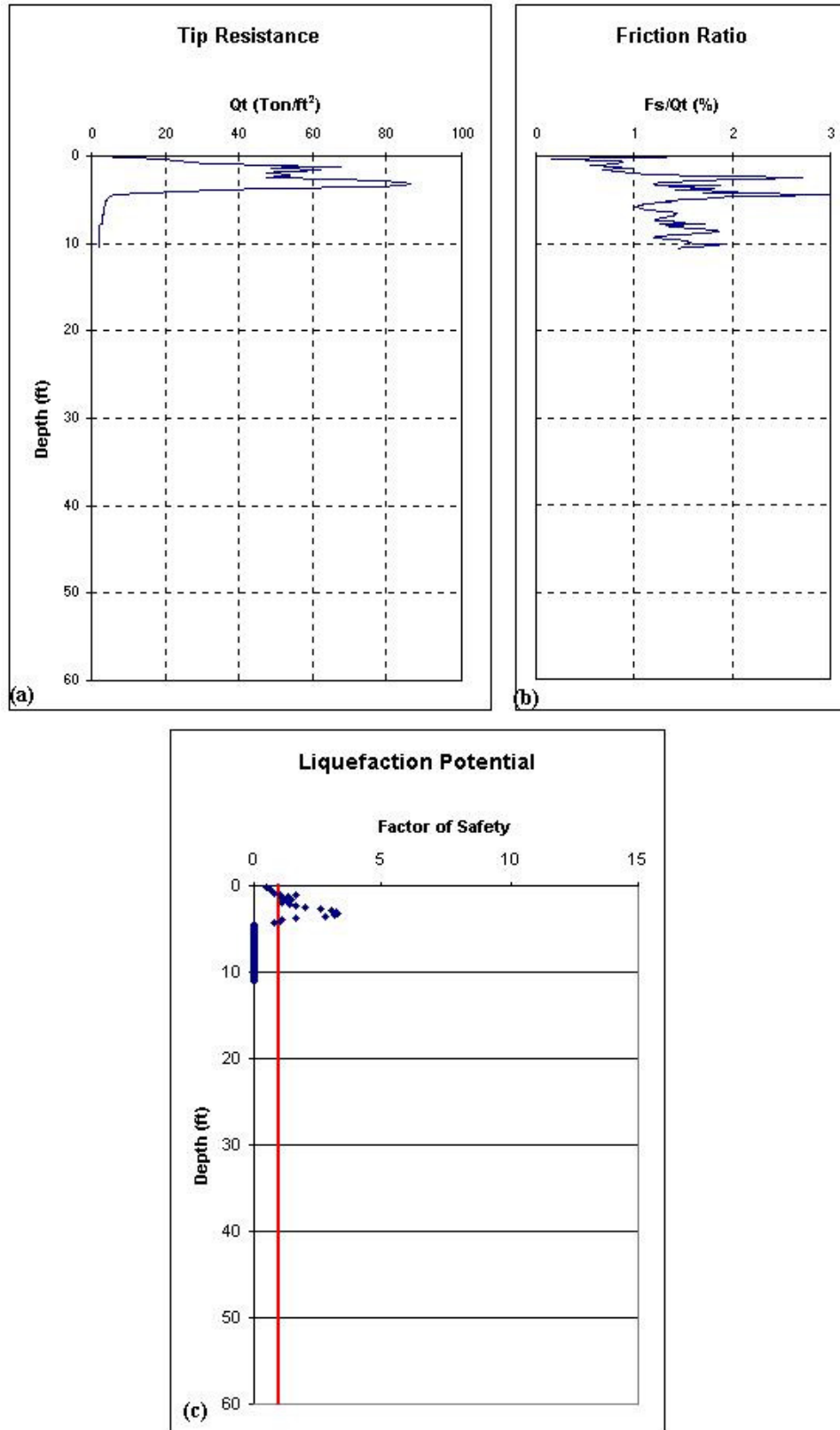


Figure 4-17: CPT-77 used in liquefaction evaluation. (a) Tip resistance, (b) Friction ratio, and (c) Liquefaction potential.

Only one boring with Standard penetration tests was drilled at the Port of Olympia. The SPT blowcounts were analyzed and the results are presented in Figure 4-18.

Hammer Type	Depth (Z) (ft)	N	r_d	σ_{ve} (psf)	σ'_{ve} (psf)	CSR	$(N_1)_{60}$	FS
Auto	4.5	9	0.969	540.00	540.00	0.151	10	0.946
Auto	6	4	0.958	720.00	720.00	0.149	4	0.530

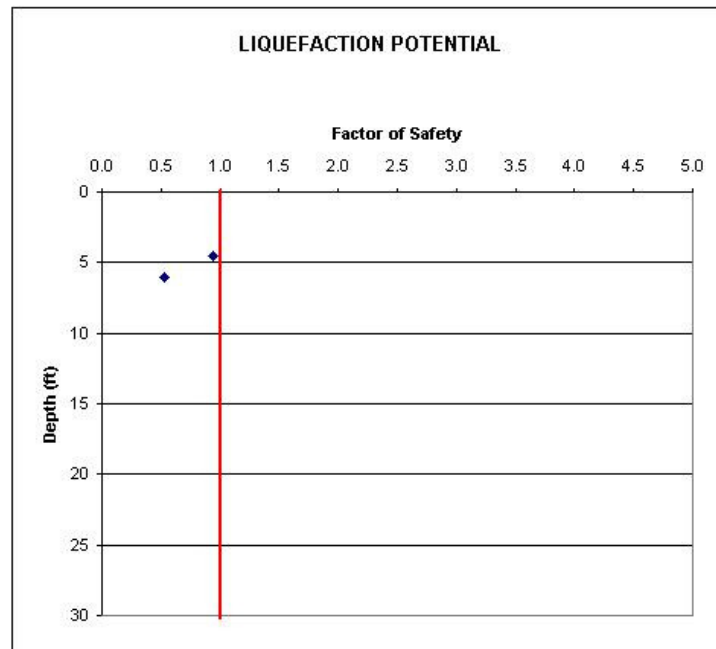


Figure 4-18: Results of SPT liquefaction analysis for boring Port of Olympia 2 (PO2).

This boring also shows a good correlation with the CPT analysis, though the water table depth at this site was found at 7 feet and these tests were performed above the water table. This makes it impossible to liquefy unless the water table depth varies seasonally.

4.4 Martin Way

4.4.1 Site Description

The Martin Way site is an earth embankment located on Martin Way, Olympia between Mary Elder Road and Ensign Road. It is a non-divided four-lane highway sloping down on the westbound direction. The embankment is around 25 to 30 feet deep along a section of about 800 feet long. The crest width was approximately 80 feet and the side slopes were around 1.5H:1V. Figure 4-19 shows the location of the site. A small natural wash crosses at the bottom of the embankment.

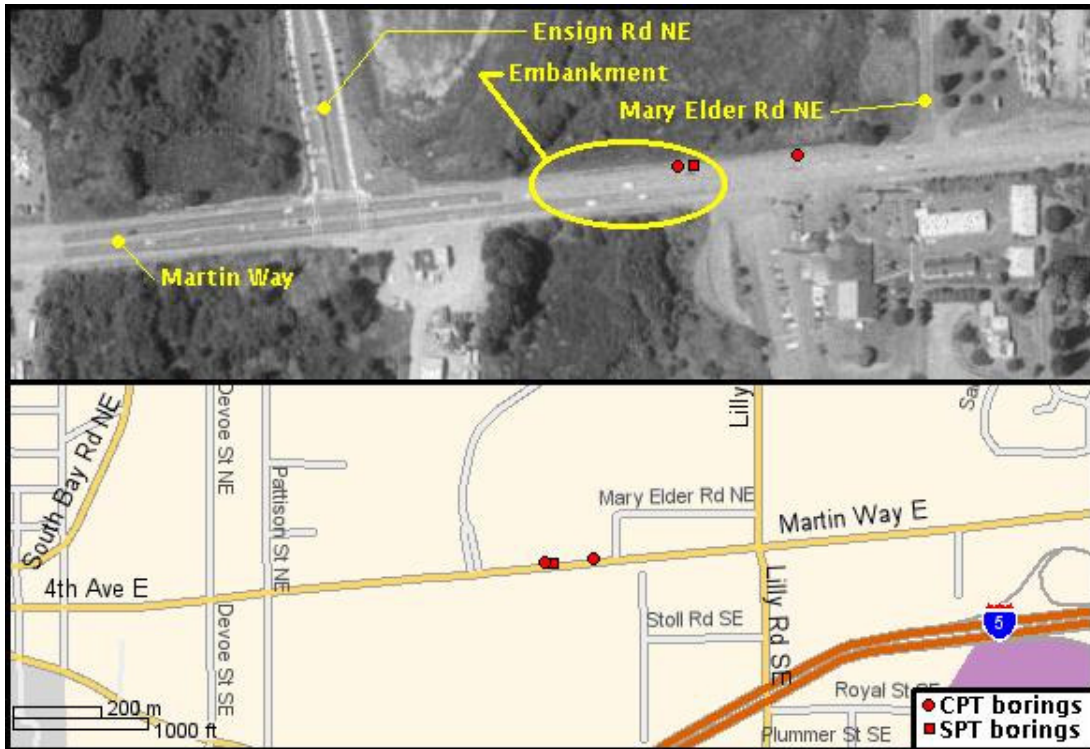


Figure 4-19. Location map and aerial picture of the Martin Way site

4.4.2 Observations of earthquake effects

Both the north and south side of Martin Way experienced lateral spreading after the earthquake as seen in Figure 4-20, though the north side was more severely damaged.



Figure 4-20. Westbound view of failed embankment on Martin Way, Olympia

4.4.3 Subsurface soil conditions and Liquefaction Evaluation

This earth embankment is primarily constructed of silty sands, although several seams of gravelly sands were found while drilling. No samples were able to be recovered from the top 20 feet, but the cone penetration test allowed to create the soil profile shown in Figure 4-21. In the first few Standard penetration tests, a catcher was used to try to retrieve samples from the embankment though no samples were being recovered. This continued until 20 feet. After this the catcher was removed and samples started being recovered. The samples retrieved throughout the profile were all silty sands. It is thought that the catcher was breaking the samples before they went in, and when the sample was pulled out of the hole the moist sandy material just would not stay in.

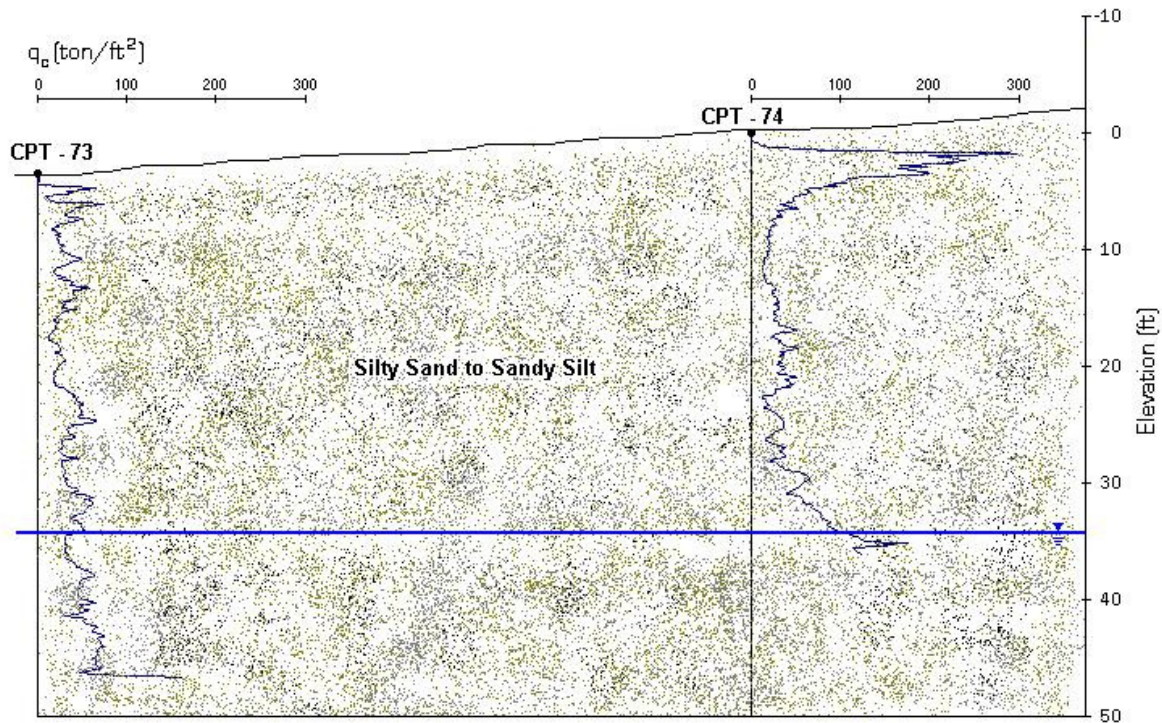


Figure 4-21. Subsurface cross-section at Martin Way, Olympia

The Martin Way embankment has a thickness of about 25 to 30 feet and is founded directly on the adjacent natural topography. The depth to the water table depth was found to be about 35 feet below the top of the embankment and hence, the water table was fairly shallow in the areas adjacent to the embankment. As mentioned before, the soil samples recovered from depths of 20 to 40 feet show that the embankment was made with a silty sand (SM) containing at least 20% fines. These fines were analyzed and they turned out to be completely nonplastic.

The liquefaction analysis results are shown below. Two CPT and one SPT borings were performed at this site.

The GPS coordinates for the CPT borings performed at Martin Way are shown in Table 4-3.

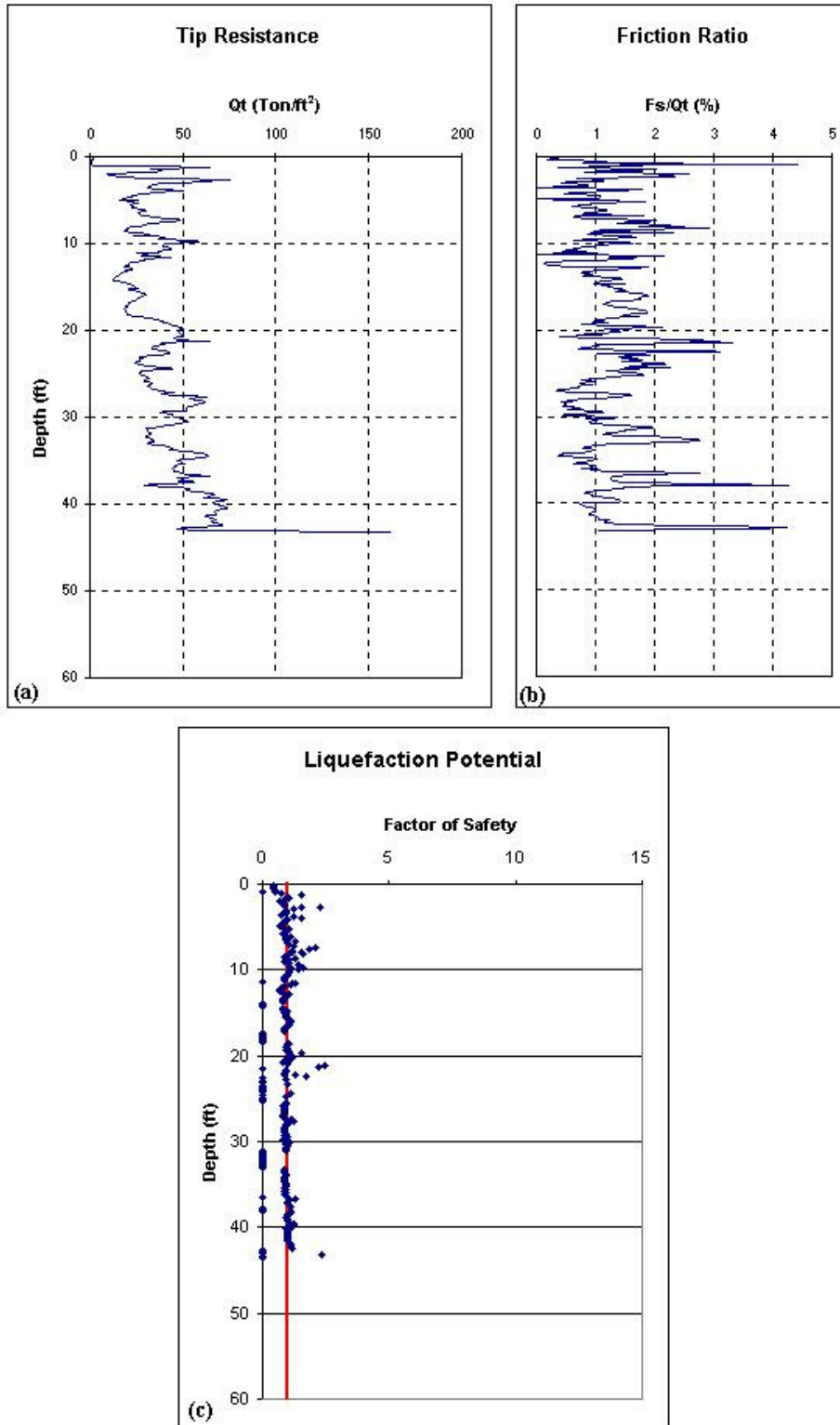


Figure 4-22: CPT-73 used in liquefaction evaluation. (a) Tip resistance, (b) Friction ratio, and (c) Liquefaction potential.

Table 4-2: GPS coordinates of CPT borings for the Port of Olympia site.

Boring No.	Position	
	Latitude	Longitude
CPT - 73	N 47 02.818	W 122 51.025
CPT - 74	N 47 02.820	W 122 50.978

* Formats: Lat/Lon ddd° mm.mmm'

Figure 4-22 shows the results for CPT-73. The results show a number of liquefiable layers although most of them are not really possible since they are above the water table. This site performed poorly during the earthquake though liquefaction may have not been the reason of failure for this site. The embankment was not brought up by compacting layer after layer. Dumping soil from the top over and over until the embankment was created made this embankment. Figure 4-23 shows a sketch of how the embankment was built.

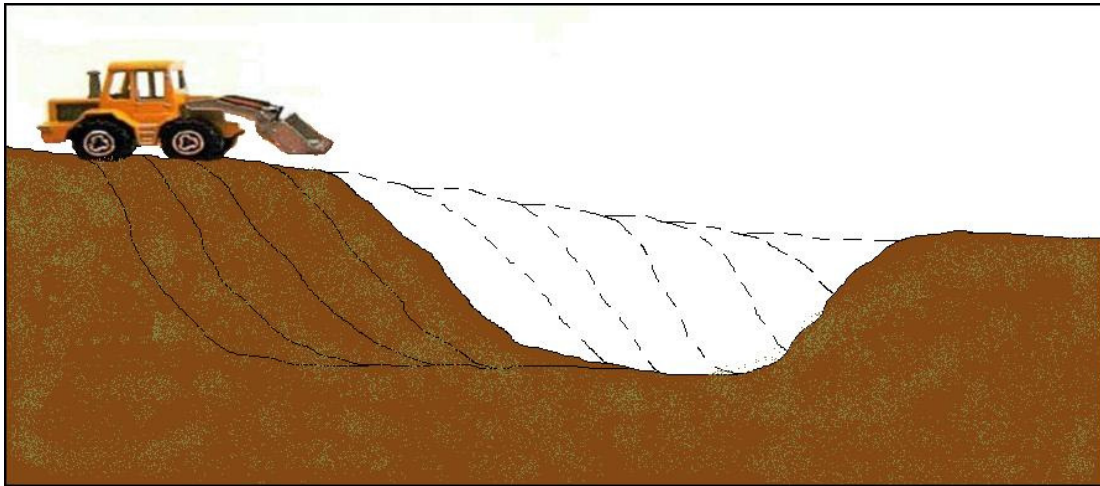


Figure 4-23: Sketch of embankment construction method.

The way this embankment was built makes believe that this failure was just a slope stability problem due to seismic loading instead of a case of liquefaction. The poor compaction methods used at the time of construction resulted in loose, contractive embankment. This is likely the cause of the stability problem in the embankment and in itself, is not considered to be a significant finding.

The liquefaction analysis performed from the CPT tests result in a high possibility of liquefaction. As seen in Figures 4-22 and 4-24, both profiles show that liquefaction should have occurred in this embankment. Looking at the water table depth this is not possible.

An SPT analysis was also performed. Results are shown in Figure 4-25. The results illustrate a low factor of safety against liquefaction along most of the profile. These results correlate very well with the CPT results although it is not correct to state that liquefaction did occur at this site since the embankment is not below the water table. With the liquefaction analysis performed on this site and the field evidence recovered

after the earthquake it can be said that this was not a case of liquefaction, and more evident a case of slope stability under seismic loading.

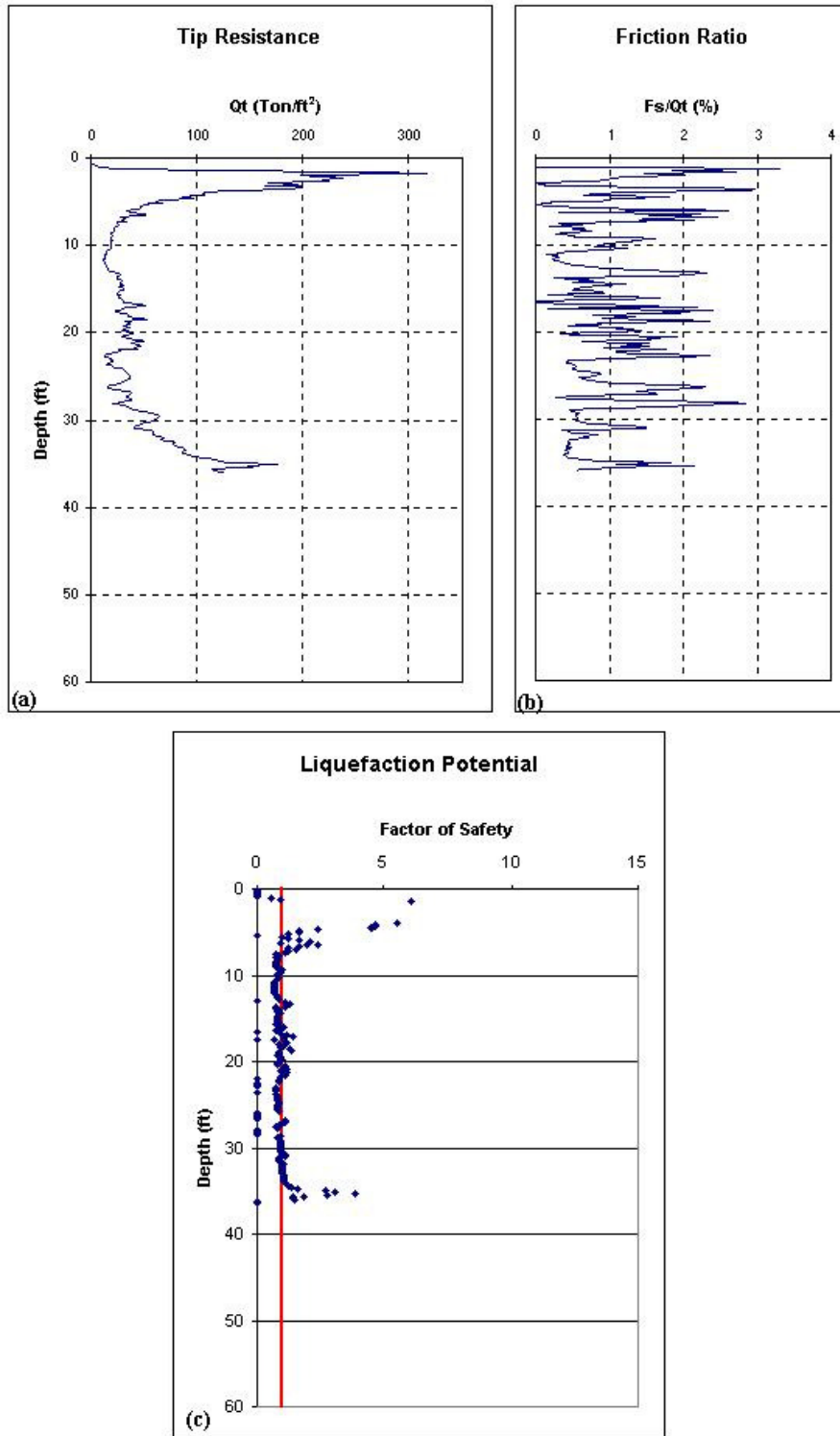


Figure 4-24: CPT-74 used in liquefaction evaluation. (a) Tip resistance, (b) Friction ratio, and (c) Liquefaction potential.

Hammer Type	Depth (Z) (ft)	N	r_d	σ_{ve} (psf)	σ'_{ve} (psf)	CSR	$(N_1)_{60}$	FS
Auto	6	4	0.958	720.00	720.00	0.149	11	1.036
Auto	11	5	0.883	1320.00	1320.00	0.138	10	1.038
Auto	16	8	0.728	1920.00	1920.00	0.114	13	1.582
Auto	21	5	0.598	2520.00	2520.00	0.093	7	1.169
Auto	23.5	4	0.559	2820.00	2820.00	0.087	5	1.014
Auto	26	7	0.532	3120.00	3120.00	0.083	9	1.582
Auto	31	7	0.496	3720.00	3628.12	0.079	8	1.512
Auto	33.5	5	0.483	4020.00	3772.12	0.080	6	1.226
Auto	36	5	0.471	4320.00	3916.12	0.081	6	1.215
Auto	38.5	8	0.461	4620.00	4060.12	0.082	9	1.605
Auto	41	17	0.452	4920.00	4204.12	0.083	19	3.203

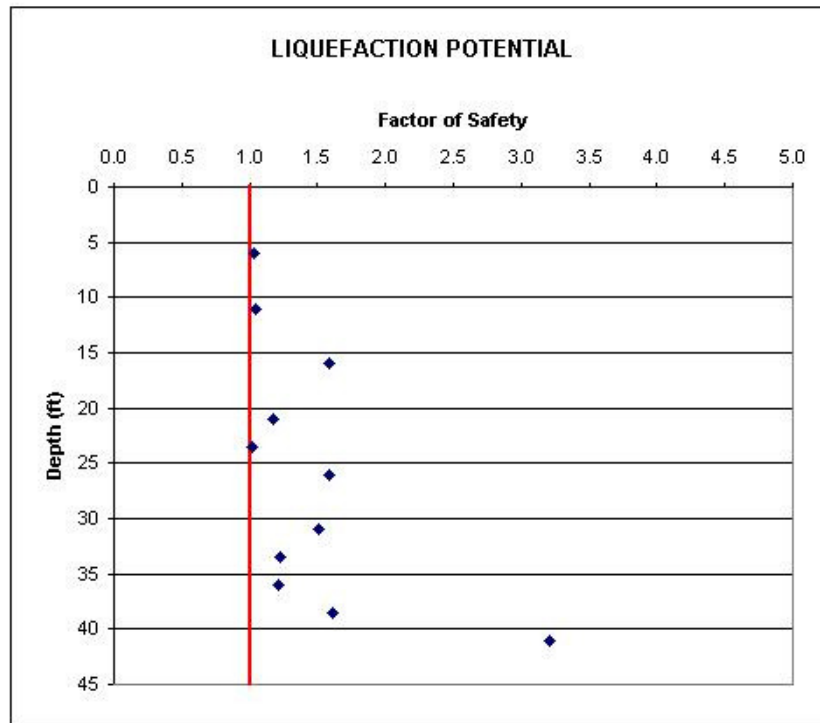


Figure 4-25: Results of SPT liquefaction analysis for boring Martin Way.

CHAPTER 5: CONCLUSIONS

A case-history study of liquefaction-related effects of three sites in the Seattle/Olympia area during the 2001 Nisqually earthquake was presented. In general, the study provided further data for the liquefiable zoning in the area. This study also brought up some interesting future research ideas discussed later in this chapter.

The south Seattle site performed poorly during the earthquake. Evidence of liquefaction was found all over the Sodo area in downtown Seattle. Of interest was a small block where structural performance varied greatly from building to building. Very loose sands underlie the site. The results show that great layer of liquefiable material underlies the site. A critical liquefiable layer was discovered from about a depth of 14 feet to about a

depth 17 feet directly under the building that had moderate performance during the earthquake. Also, one boring was made (CPT-70) south of this site where the buildings performed poorly. The results for this boring (Figure 4-7) show that this critical liquefiable layer does not appear, although this boring was only 110 feet away from the test site. This indicated that maybe liquefaction had to do something with the performance of the buildings. If a layer has liquefied, it might dissipate some of the energy from the shear waves of the earthquake, creating a natural base isolation system that would enable a fair performance in the structures above. This might be one of the reasons why structural performance varied greatly along this block.

The Port of Olympia site is underlain with a five to eight feet thick layer of sandy gravel to gravelly sand. This material was placed through hydraulic fill. This method of fill placement should not be used in seismic regions where native soils include clean sands or silty sands. The main reason why these type of sites tend to liquefy is because no compaction technique is applied at the time of construction so the material tends to be loose and very susceptible to liquefaction. The Port suffered more damage toward the north part of the site (near CPT-71 and CPT-72). The silty sand to sandy silt layer found toward the north side of the site at about a depth of 8 to 12 feet was the most probable cause of liquefaction.

The Martin Way embankment between Mary Elder Rd. and Ensign Rd. did not yield clear results concerning the liquefaction potential of the site. Soil samples were recovered from this site and tested. The results show that the soils could liquefy given the right circumstance but most of the soils that show a low factor of safety against liquefaction (Figures 4-22 and 4-24) are above the water table. With this in mind two possibilities come into picture. One: no liquefaction occurred at this site and the failure was caused by a slope stability failure due to the bad construction method of the embankment. And two: Liquefaction occurred down at the native soils making the toe of the slope weak, therefore causing the slope failure. The more probable conclusion based on the facts and the analyses performed would be to say that no liquefaction occurred at this site and that it was more a slope failure problem.

One of the conclusions to this investigation is that no liquefaction analysis based on CPT tests should be performed without the appropriate samples retrieved in order to confirm the soil properties and classification. All of the soils encountered at this site were analyzed using the CPT data for liquefaction evaluation analysis. If only the analysis spreadsheets would have been used, the results would have showed that most of the soils were too clay rich to liquefy. This is not the case since all of the soils turned out to be liquefiable. In order to determine this, soil samples need to be retreated and analyzed. In order to be able to say for sure that the soil is too clay rich to liquefy, the “Chinese Criteria”, explained earlier on Chapter 3, has to be met. This criterion determines how clay rich are the fines content of the sample. This is very important since the amount of fines does not determine the liquefaction potential, but the clay percentage found in the fines.

When performing Standard penetration tests for liquefaction analysis purposes, very careful assumptions should be made about the hammer energy transfer ratio (ER). The ER when doing the corrections for calculating $N_{1(60)}$ have a great effect on the results. If no dynamic analysis is made at the time of drilling, it is practical to assume that 60

percent of the energy is transferred to the sampler not depending on the hammer type. Two different situations were encountered in this study. The first one is hammer type. Two different hammers were used to perform the Standard penetration tests. When the Rope and Cathead cylinder hammer was used, the energy readings had an average of 41%. There are different theories on why the energy was so low. One of them could have been the humidity of the rope, or the friction in the pulley system. With the auto-trip hammer the average energy readings were 98% having some that went over 100%. The hammer was then examined and it was determined that this specific hammer had a drop height of about 35 inches and an impact velocity of 14.03 feet per seconds. This determined that when we are getting ER's over 100%, we are comparing a hammer weighing 140 pounds and dropping 30 inches to the same hammer dropping 35 inches. This was the source for the high ER's when using the auto-trip hammer system. With the energy measurements a good correction was made for the SPT blowcounts. If no energy readings would have been taken, most probably the assumption that 60% of the energy was being transmitted would have been used. The results would have indicated that the materials have an even higher potential for liquefaction than actual. While this could be thought of as a conservative deviation, it also creates situations where significant time and expense is spent on unnecessary mitigation of project sites.

It is hoped that the data and results presented in this paper will contribute to the further development of semi empirical correlations for predicting liquefaction potential on soils. Where liquefaction studies are of primary concern, additional research that provides on-board instrumentation to drill rigs during standard penetration resistance testing would be helpful to the industry.

ACKNOWLEDGEMENTS

This work was sponsored by the United States Geological Survey, Grant No. 02HQGR0015. Acknowledgement is made of the coauthors of this report, including Mr. Vasco Duke, who earned his Master of Science in Civil Engineering degree at The University of Arizona with this support, and Mr. Juan Lopez, who completed an undergraduate research thesis through the project. Their assistance is greatly appreciated.

REFERENCES

- American Society for Testing and Materials (ASTM) (1996). "Standard Practice for Determining the Normalized Penetration Resistance of Sands for Evaluation of Liquefaction Potential, D6066-96, ASTM, Philadelphia, PA.
- Bray, J.D., Sancio, R.B., Kammerer, A.M., Merry, S.M., Rodriguez-Marek, A., Khazal, B., Chang, S., Bastani, A., Collins, B., Hausler, E., Dreger, D., Perkins, W.J., and Nykamp, M. (2001). "Some Observations of Geotechnical Aspects of the February 28, 2001, Nisqually Earthquake in Olympia, South Seattle, and Tacoma, Washington." Pacific Earthquake Engineering Research Center, <http://peer.berkeley.edu/publications/nisqually/geotech/index.html>.
- Liao, S., and Whitman, R.V. (1986). "Overburden Correction Factors for SPT in Sand." *Journal of Geotechnical Engineering*, ASCE, Vol. 112, No. 3, March, pp. 373–377.

- Robertson, P.K., and Wride, C.E. (1998). "Evaluating Cyclic Liquefaction Potential Using the Cone Penetration Test." *Canadian Geotechnical Journal*, Ottawa, Vol. 35, No. 3, pp. 442–459.
- Seed, H. B. (1979). "Soil liquefaction and cyclic mobility evaluation for level ground during earthquakes." *Journal of the Geotechnical Engineering Division, ASCE*, Vol. 105, No. 2, pp. 201–255.
- Seed, R. B., Dickenson, S. E., Rau, G. A., White, R. K., and Mok, C. M. (1994). "Site effects on strong shaking and seismic risk: Recent developments and their impact on seismic design codes and practice." *Proceedings of the Structural Congress II*, Vol. 1, ASCE, New York, pp. 573–578.
- Seed, H. B., and Idriss, I. M. (1971). "Simplified procedure for evaluating soil liquefaction potential." *Journal of the Geotechnical Engineering Division, ASCE*, Vol. 97, No. 9, pp. 1249–1273.
- Seed, H. B., and Idriss, I. M. (1982). "Ground motions and soil liquefaction during earthquakes." *Earthquake Engineering Research Institute Monograph*, Oakland, Calif.
- Seed, H. B., Tokimatsu, K., Harder, L. F., and Chung, R. M. (1985). "The influence of SPT procedures in soil liquefaction resistance evaluations." *Journal of the Geotechnical Engineering Division, ASCE*, Vol. 111, No. 12, pp. 1425–1445.
- Skempton A.K. (1986). "Standard Penetration Testing Procedures and the Effects in Sands of Overburden Pressure, Relative Density, Particle Size, Aging, and Overconsolidation." *Geotechnique*, London, Vol. 36, No. 3, pp. 425–447.
- Stark, T.D. and Olson, S.M. (1995). "Liquefaction Resistance Using CPT and Field Case Studies." *Journal of Geotechnical and Geoenvironmental Engineering, ASCE* Vol. 121, No. 12, December, pp. 856–869.
- Suzuki, Y., Tokimatsu, K., Koyamada, K., Taya, Y., and Kubota, Y. (1995). "Field Correlation of Soil Liquefaction Based on CPT Data." *Proc., Int. Symp. on Cone Penetration Testing*, Vol. 2, pp. 583–588.
- Youd, T.L., Idriss, I.M., Andrus, R.D., Arango, I., Castro, G., Christian, J.T., Dobry, R., Finn, W.D. Liam, Harder, Jr., L.F., Hynes, M.E., Ishihara, K., Koester, J.P., Liao, S.S.C., Marcuson, III, W. F., Martin, G.R., Mitchell, J.K., Moriwaki, Y., Power, M.S., Robertson, P.K., Seed, R.B., and Stokoe, II, K.H. (1997) "Liquefaction Resistance of Soils: Summary Report from the 1996 NCEER and 1998 NCEER/NSF Workshops on Evaluation of Liquefaction Resistance of Soils," *Journal of Geotechnical and Geoenvironmental Engineering, ASCE* Vol. 127, No. 10, October, pp. 817–833.